ANL-HEP-CP-82-72
December, 1982
Conf-8210107--4

HADRONIC PRODUCTION OF MASSIVE LEPTON PAIRS*

ANL-HEP-CP--82-72
DE83 008928

Edmond L. Berger
High Energy Physics Division
Argonne National Laboratory
Argonne, IL 60439

ABSTRACT

A review is presented of recent experimental and theoretical progress in studies of the production of massive lepton pairs in hadronic collisions. I begin with the classical Drell-Yan annihilation model and its predictions. Subsequently, I discuss deviations from scaling, the status of the proofs of factorization in the parton model, higher-order terms in the perturbative QCD expansion, the discrepancy between measured and predicted yields (K factor), high-twist terms, soft-gluon effects, transverse-momentum distributions, implications for weak vector boson ($W^{\pm}$ and Z°) yields and production properties, nuclear A dependence effects, correlations of the lepton pair with hadrons in the final state, and angular distributions in the lepton-pair rest frame.

I. INTRODUCTION

I hope to accomplish two aims in my role as the first speaker at this Workshop. I intend to review briefly the salient phenomenology of massive lepton pair production[1,2] and the interpretation of the experimental observations in terms of the classical Drell-Yan annihilation model.[3] Second,

*Invited review presented at the Fermilab Workshop on Drell Yan Processes, Fermilab, October, 1982.

in order to place the proceedings of the next two days into context, I will try to touch on most of the topics which will be addressed in detail by subsequent speakers. My intent in this second portion of the lecture is not to provide answers but to stimulate questions. Some of these questions will be answered, at least in part, during our Workshop. Others will require new experiments and theoretical developments. Massive lepton pair production is recognized for the important and relatively clean tests which it offers of many parton model and quantum chromodynamics (QCD) concepts and computations. Correspondingly, much of the discussion in this Workshop is relevant directly to all hard-scattering processes initiated by the interaction of two incident hadrons.

In Section II, I present the classical annihilation model,[3] and I summarize some of its principal expectations, along with a survey of relevant data. Incorporated in this model is a strong assumption that all long-distance, long-time scale "soft" hadronic effects in the initial state may be absorbed into process independent, factorized probabilities, the incident parton distribution functions. This assumption has been questioned recently; I will describe the state of this "factorization controversy" in Sec.III. In Sec.IV, I review the impact of higher order QCD contributions on predictions for the absolute yield of massive lepton pairs. Experimental and theoretical discussions of absolute normalization are usually presented in terms of a "K-factor". This factor is defined in Sec.IV, and a summary is presented of experimental information available on the magnitude of K and its dependence on kinematic variables. High twist contributions are discussed briefly in Sec.V. The process $\pi^- N \to \gamma^* X$ is especially useful for constraining the size and kinematic behavior of such contributions. Transverse momentum spectra are

addressed in Sec.VI, with special emphasis placed on recent attempts to incorporate soft gluon radiation. In passing, in various places in the text, I shall mention implications for weak vector boson ($W^{\pm}$ and Z°) yields and production properties, nuclear A dependent effects, correlations of the lepton pair with hadrons in the final state ("associated hadrons"), and angular distributions in the lepton pair rest frame.

II. CLASSICAL ANNIHILATION MODEL

In the parton model proposal of Drell and Yan, the massive virtual photon (γ^*) in the reaction $h_a h_b \to \gamma^* X$ is produced by a point-like annihilation of a quark from one initial hadron with an antiquark from the other.[3] The photon materializes as a massive lepton pair: $q\bar{q} \to \gamma^* \to \ell^+\ell^-$. Both initial partons are on or near the mass shell. The process is sketched in Fig.1. The impulse approximation, point-like coupling embodied in Fig.1 should be valid for large enough $M_{\ell\bar{\ell}}$; e.g. $M_{\ell\bar{\ell}} \gtrsim 4$ GeV. The model applies only to the lepton pair continuum, not to the production of vector meson resonances such as the J/Ψ and Υ.

The variables x_i denote the fractional longitudinal momenta of the partons, and $\vec{k}_T$ is a small "intrinsic" transverse momentum of the parton with respect to the collinear axis defined by the initial hadrons. Process independent quark and antiquark parton densities, $q(x,k_T)$ and $\bar{q}(x,k_T)$, are assumed to represent all long-distance long-time scale hadronic physics, such as the binding of partons within hadrons and whatever initial state interactions may have taken place between the initial hadrons. These densities were assumed originally to be scale independent, i.e. not to depend

on $M^2_{\ell\bar{\ell}}$. The model provides normalized predictions for the γ^* production cross section multiply differential in M^2, in the scaled longitudinal momentum x_F of the γ^*, in the transverse momentum p_T of the γ^*, and in the decay angles (θ^*,ϕ^*) in the γ^* rest frame:

$$\frac{d^5\sigma(h_a h_b \to \gamma^* X)}{dM^2 dx_F dp_T^2 d\cos\theta^* d\phi^*} .$$

Statements of at least a qualitative nature may also be made about the expected properties of the associated hadronic system, X, as a function of M^2, x_F, p_T^2 and the type of beam and target.

When integrated over the transverse momentum of the massive lepton pair and over decay angles in the $(\ell\bar{\ell})$ rest frame, the cross section predicted in the classical model is

$$\frac{d^2\sigma}{dM^2 dx_F} = \frac{4\pi\alpha^2}{9sM^2} \frac{1}{(x_1 + x_2)} \sum_f e_f^2 [q_f(x_1)\bar{q}_f(x_2) + (1 \leftrightarrow 2)] . \qquad (1)$$

Here $M^2 = sx_1x_2$, and the fractional longitudinal momentum of the γ^* is

$$x_F = \frac{2p_L(\gamma^*)}{\sqrt{s}} = x_1 - x_2 . \qquad (2)$$

In Eq.(1), α is the usual electroweak coupling strength $\alpha \cong 1/137$; e_f denotes the fractional charge of the quark of flavor f; and $q_f(x_1)$ is the quark density, integrated over the intrinsic k_T. These $q_f(x)$ are presumed to have been measured elsewhere, for example, in deep inelastic lepton scattering experiments. The numerical factor 1/9 in Eq.(1) includes a color factor 1/3 which expresses the statement that only quarks and antiquarks of a given color

may annihilate electromagnetically.

Embodied in Eq.(1) is the assumption of strong factorization, to which I shall return in Sec.III. Second, a direct consequence of Eq.(1) is the prediction of scaling:

$$\frac{M^4 d\sigma}{dM^2 dx_F} = f(\tau, x_F) \ . \tag{3}$$

Here, $\tau = M^2/s$.

A. Higher Order Processes in QCD.

Before discussing the extent to which present data satisfy Eq.(3), I want to review QCD "improvements" to the annihilation model and their implications for deviations from scaling.

In addition to the zero-th order Born subprocess, $\bar{q}q \to \gamma^*$, sketched in Fig.2(a), QCD perturbation theory requires that we consider many other contributions to γ^* production. Many diagrams can be drawn, with initial state or final state gluons attached to various quark and antiquark lines. Some of these are sketched in Fig.2(b)-(h). The basic validity of the parton model is assumed. In particular, it is taken for granted that we can define process-independent quark, antiquark, and gluon structure functions, and that it is meaningful to isolate short-distance hard-scattering subprocesses. In some of the subprocesses sketched in Fig.2, the initial state is a quark-antiquark system, as for the Born subprocess, Fig.2(a). However, for most of the higher order subprocesses the initial state is instead qq, qG, $\bar{q}$G, or GG.

If these higher order QCD subprocesses are important, to what extent is it meaningful physically to continue to refer to massive lepton pair

production as a quark-antiquark annihilation process, i.e. as "the Drell-Yan process"? If quark-quark and quark-gluon subprocesses are important in the hadroproduction of massive lepton pairs, may the data be used to extract quark and antiquark structure functions for comparison with similar functions derived from deep inelastic lepton scattering experiments?

Answers to these and related questions are provided by a detailed analysis of the contributions of the QCD subprocesses sketched in Fig.2, in parallel with analogous analyses of corresponding QCD contributions to deep inelastic lepton scattering (DIS). Parallel examination of deep inelastic scattering is necessary because the quark and antiquark probabilities $q(x,Q^2)$, $\bar{q}(x,Q^2)$, which we want to use, are defined in terms of the observed DIS structure functions $F_2(x,Q^2)$ and $F_3(x,Q^2)$.

I will summarize the results of the analyses alluded to above. Let us focus attention on the lepton pair cross section $d^2\sigma/dM^2dx_F$, integrated over $p_T(\gamma^*)$. For a given order, n, in a perturbation expansion in the strong coupling α_s, the contribution of QCD subprocesses to $d^2\sigma/dM^2dx_F$ may be expanded in a power series in $\ell n(M^2)$:

$$\sigma_n = \alpha_s^n[a_n(\tau,x_F)\ell n^n(M^2) + b_n\ell n^{n-1}(M^2) + \ldots] \ . \qquad (4)$$

For each order in perturbation theory, the leading logarithm approximation consists in retaining only the first term in this series--i.e. only the term with the largest power of $\ell n(M^2)$ in Eq.(4). In this leading log approximation, it may be shown[4] that the prediction for $d^2\sigma/dM^2dx_F$, after including higher order QCD subprocesses, is equal to the classical Drell-Yan formula, Eq.(1), provided one uses the scale dependent parton densities

defined in DIS:

$$q_f(x) \to q_f^{DIS}(x,M^2) \ ; \tag{5a}$$

$$\bar{q}_f(x) \to \bar{q}_f^{DIS}(x,M^2) \ ; \tag{5b}$$

and

$$M^2 = |Q^2|_{DIS} \quad . \tag{5c}$$

More explicitly, at the leading log level in QCD, Eq.(1) is replaced by

$$\frac{d^2\sigma_{\text{lead log}}}{dM^2 dx_F} = \frac{4\pi\alpha^2}{9sM^2} \frac{1}{(x_1+x_2)} \sum_f e_f^2 [q_f(x_1,M^2)\bar{q}_f(x_2,M^2) + (1\leftrightarrow 2)] \ . \tag{6}$$

This remarkable result restores the full predictive power of the classical model, at least when M^2 is large enough to justify neglect of the next-to-leading terms in Eq.(4). It need not have been true theoretically that perturbative QCD would justify the classical annihilation model as the correct "Born term". Beyond the leading log approximation, there are important residual contributions, some of which I'll discuss in Sec.IV. These residual contributions may be very large especially near the edges of phase space: $\tau \to 1$, or $x_F \to 1$.

B. Scaling and Deviations from Scaling.

Specific deviations from scaling are implied by Eq.(6). By restricting attention to regions of phase space away from various kinematic limits, i.e. by choosing values of x_i, τ, and x_F sufficiently distant from their kinematic

limits, we can presumably safely ignore high-twist inverse-power ($1/M^2$) contributions to scaling deviations in both DIS and massive lepton pair production. Because the parton densities in Eq.(6) depend logarithmically on M^2 at fixed x, Eq.(3) is replaced by

$$\frac{M^4 d\sigma}{dM^2 dx_F} = \tilde{f}(\tau, x_F, \ell n(M^2/\Lambda^2)) \ . \tag{7}$$

In the range explored experimentally, $0.1 \lesssim M/\sqrt{s} \lesssim 0.5$, with $20 \text{ GeV} \lesssim \sqrt{s} \lesssim 60 \text{ GeV}$, the expected leading log scaling violations are small. This point is illustrated in Fig.3a. I used the 1982 structure functions determined by the CERN-Dortmund-Heidelberg-Saclay collaboration[5] from fits to their neutrino and antineutrino data. For $pN \to \gamma^* X$ at $(M/\sqrt{s}) = 0.5$, a factor of two decrease is predicted in the quantity $sd^2\sigma/dy\, d\sqrt{\tau}$ when the lepton pair mass is changed from M = 10 GeV to M = 30 GeV. Here y is the rapidity of the γ^*. Near $(M/\sqrt{s}) = 0.15$, an increase of the cross section by a factor of 1.25 is expected. Essentially no scaling deviations are expected for $M/\sqrt{s}$ in the range 0.20 to 0.25. In Fig.3b, I compare leading log expectations for $pp \to \gamma^* X$ at $\sqrt{s} = 60$ GeV and $\sqrt{s} = 800$ GeV. At $M/\sqrt{s} = 0.05$, a gain of about 2.5 is foreseen in the scaling cross section when the energy is increased from the ISR range to that of Brookhaven's CBA. I do not have enough confidence in the structure functions to extend these predictions to $\sqrt{s} = 2$ TeV. Note that I have not included production of the Z° in the computations.

In Fig.3c I present computations for $\bar{p}p \to \gamma^* X$. These predictions are much less sensitive to systematic uncertainties[5] in our knowledge of the sea quark distributions. Again, essentially no deviations from perfect scaling

are foreseen in the neighborhood of $M/\sqrt{s} = 0.2$. At $\sqrt{s} = 60$ GeV and $y = 0$, the ratio of cross-sections $\sigma(\bar{p}p \to \gamma^* X)/\sigma(pp \to \gamma^* X)$ rises from roughly 3 at $M/\sqrt{s} = 0.10$, to about 10 at $M/\sqrt{s} = 0.25$, and to roughly 100 at $M/\sqrt{s} = 0.45$. My calculations indicate that this ratio is to a good approximation a function only of $M/\sqrt{s}$, with very little residual dependence on $\sqrt{s}$. According to our current understanding of next-to-leading log contributions, the $\bar{p}p/pp$ ratio should not be affected by the physics of the K factor discussed in Sec.IV.

Precise tests of scaling require data at fixed $M/\sqrt{s}$ over a broad range of $\sqrt{s}$. Present tests are limited by systematic effects and because the range of values of $M/\sqrt{s}$ explored in fixed target experiments at Fermilab and CERN differs from that studied at the CERN ISR. The data in Fig.4 show that in both $pN \to \gamma^* X$ and $\pi^- N \to q^* X$, scaling is verified to within 25% over the range $0.1 < M/\sqrt{s} < 0.6$. This result is important because it indicates that massive lepton pair production is controlled by a pointlike subprocess. By contrast, for whatever reasons, such simple dimensional scaling is not observed in the "large p_T" hadroproduction of pions at the values of p_T accessible now in fixed target experiments at Fermilab and CERN. The massive lepton pair data are not yet of sufficient precision to allow tests of deviations from scaling.

C. Magnitude and Shape of Cross Sections.

Provided that the quark and antiquark structure functions are known, the absolute magnitude of the cross section and its functional dependence on M^2 and x_F are predicted exactly by Eq.(6). For some years, agreement of experiment and theory on the absolute rate was advertised as a good way to measure the number of colors, N_c. It has now been established that the experimental yield is roughly a factor of two greater than predicted by

Eq.(6), with $N_c = 3$, at least over the relatively narrow range of values of M^2, x_F and s studied thus far. This situation and its interpretation are described in more detail in Sec.IV. If we can ignore the M and x_F dependences of the K factor discussed in Sec.IV, the M and x_F dependences of $d^2\sigma/dM^2dx_F$ allow us to check whether the structure functions which control $pN \to \gamma^*X$ are the same as those measured in deep inelastic lepton scattering.

Measurements of $\bar{p}p \to \gamma^*X$ have long been regarded as especially significant for testing the basic validity of the annihilation model. The cross section is predicted with a high degree of confidence because it is a convolution of valence quark distributions, $q_p(x,M^2) = \bar{q}_{\bar{p}}(x,M^2)$, which are determined well in deep inelastic lepton scattering. Recent developments in both theory and experiment indicate that the dynamics of hard scattering processes are becoming more complex. These developments include the anomalous A dependence in the deep inelastic lepton cross section and its likely association with sea quarks (Sec.II.E), controversies associated with non-factorization (Sec.III), and large "corrections" in next-to-leading order $(K(x_1,x_2)$, Sec.IV). For these reasons the importance of investigations with antiprotons is substantially enhanced. I hope excellent data will be obtained before the CERN ISR are retired.

D. Structure Functions.

If Eq.(6) is assumed, data from $hN \to \gamma^*X$ can be used to determine the quark and antiquark structure functions of various incident hadrons, such as the π, K, and the photon. As discussed in Sec.IV, the presence of a large K factor complicates matters, but important qualitative or semi-quantitative checks of the annihilation model are still possible. For example, it is

observed[1] that the ratio

$$R\left(\frac{\pi}{p}\right) = \frac{\frac{d^2\sigma}{dM\,dy}(\pi^- N \to \gamma^* X)}{\frac{d^2\sigma}{dM\,dy}(pN \to \gamma^* X)} \tag{8}$$

rises rapidly with M. In the annihilation model, at large M, $R(\pi/p)$ is proportional roughly to the ratio of probabilities for finding antiquarks in the π and in the proton. Pions have valence antiquarks, whose probability is thought to behave as $\bar{q}_\pi(x) \propto (1-x)$. In the proton the antiquarks are in the sea, with $\bar{q}_p(x) \propto (1-x)^n$, $n \gtrsim 6$. Correspondingly, we may expect $R(\pi/p) \propto (1-x)^{1-n}$, with $x = M/\sqrt{s}$. In another test[1] of the annihilation picture, data are also consistent with the prediction that as M increases

$$\frac{\sigma(\pi^+ N \to \gamma^* X)}{\sigma(\pi^- N \to \gamma^* X)} \to \left(\frac{e_d}{e_u}\right)^2 = \frac{1}{4}\,. \tag{9}$$

Here N denotes an "isoscalar" target. At relatively small values of M the ratio is closer to unity, presumably because the sea quarks in the π^+ and π^- are dominant at small x_1 (and small $M/\sqrt{s}$).

A nontrivial confirmation of the parton approach to γ^* production is the experimental demonstration that the antiquark structure function $\bar{q}_\pi(x)$ behaves roughly as $(1-x)$, typical of valence antiquarks and not of the sea, and that the data show the expected valence quark charge dependence.

E. Nuclear A Dependence.

Once corrections are made for the different x dependences of the up and down quark distributions, u(x) and d(x), the cross section $hA \to \gamma^* X$ for production from a nuclear target, A, is expected to increase linearly with

A. This statement should hold for values of the fractional longitudinal momenta x_1 and x_2 not too near their kinematic limits.[10] Interesting shadowing affects may be visible if one of the x_1 is very small.[10] Massive lepton pair data[1,6] are generally consistent with the expectation of a linear A dependence for M $\gtrsim$4 GeV. On the other hand, recent data from the European Muon collaboration[11] cast doubt on our understanding of A dpendence. The structure function $F_2(x,Q^2)$ is measured in $\mu A \to \mu' X$ at large Q^2 for A = Iron and A = deuterium. An unexpected x dependent behavior is observed in the ratio $F_2^{Iron}(x,Q^2)/F_2^{D_2}(x,Q^2)$. At fairly small x, this ratio is consistent with $A^{1.06}$, but near x = 0.7 it behaves as $A^{0.94}$. These data suggest that the effective sea quark distribution is enhanced in nuclei at low x, $x \lesssim 0.25$, and that the valence quark distribution functions are depressed at larger values of x. Data on massive lepton pair production tend to be concentrated in the interval $0.2 < x < 0.5$, where the deep inelastic muon cross section shows little deviation from $A^{1.0}$. Nevertheless, it would be valuable to check more carefully whether the effective sea is also enhanced in $hN \to \mu\bar{\mu}X$. The question may be addressed by a careful comparison of $pA \to \mu\bar{\mu}X$ and $pp \to \mu\bar{\mu}X$ as a function of both x_F and M^2.

F. Transverse Momentum Spectra.

The original parton model is based on a field theory with an external cutoff in the parton transverse momenta k_T. In the classical Drell-Yan annihilation model, the transverse momentum p_T of the γ^* is provided entirely by these "intrinsic" k_T. Therefore, one would have expected that the measured mean $\langle p_T(\gamma^*)\rangle$ would be "small" ($\ll M_{\gamma^*}$) and independent of s at fixed $M/\sqrt{s}$.

However, data indicate that $\langle p_T^2\rangle$ grows with s. Various functional forms

have been used in fits to data. A simple expression with two parameters is

$$\langle p_T^2 \rangle = a + bs \ . \tag{10}$$

Both the slope, b, and the intercept, a, are expected to be functions of τ and x_F. Another favorite expression is

$$\langle p_T \rangle = c + d\sqrt{s} \ . \tag{11}$$

Given the quality of the data, either Eq.(10) or Eq.(11) provides an acceptable fit.

For $pN \to \gamma^* X$ at $M/\sqrt{s} \simeq 0.22$, one finds[12,13]

$$\langle p_T^2 \rangle = 0.52 + (1.4 \times 10^{-3})s \ , \tag{12}$$

whereas for $\pi^- N \to \gamma^* X$ at $M/\sqrt{s} = 0.28$,

$$\langle p_T^2 \rangle = 0.59 + (2.8 \times 10^{-3})s \ . \tag{13}$$

In these fits, both the intercept and the slope have probable (one-standard-deviation) errors of about 10% of their values. Data on the $\sqrt{s}$ dependence of $\langle p_T \rangle$ are summarized[12] in Fig.5 for $pN \to \gamma^* X$ at $M/\sqrt{s} = 0.22$.

In addition to their role in modifying the classical formula for $d^2\sigma/dM^2 dx_F$, discussed above, the subprocesses sketched in Fig.2 generate a p_T^{-2} tail in the γ^* transverse momentum distribution $d\sigma/dp_T^2$ at large p_T. This

implies that $\langle p_T^2 \rangle \propto s$ at fixed $M/\sqrt{s}$ and fixed x_F. The experimental growth of $\langle p_T^2 \rangle$ with s is evidence for an underlying quantum field theory of the strong interactions. In Sec.VI I will discuss in more detail the extent to which present QCD calculations provide a quantitative description of p_T spectra.

G. Angular Distributions.

Just as in $e^+e^- \to q\bar{q}$, the massive virtual photon γ^* in $q\bar{q} \to \gamma^* \to \mu\bar{\mu}$ should decay with a polar angular distribution $d\sigma/d\cos\theta \propto (1 + \cos^2\theta)$, where $\cos\theta$ is measured in the γ^* rest frame with respect to the collinear $q\bar{q}$ direction. This collinear $q\bar{q}$ axis is, of course, not controlled in $hN \to \gamma^* X$, and it is necessary to specify the angular distribution $d^2\sigma/d\cos\theta d\phi$ with respect to some suitable set of axes determined by the incident hadrons. Popular choices include the well known t-channel (Gottfried-Jackson) and s-channel helicity axes, as well as a set of axes devised by Collins and Soper.[14]

The measured polar angular distribution may be parametrized as

$$\frac{d\sigma}{d\cos\theta} \propto (1 + \alpha\cos\theta) \ . \tag{14}$$

The absolute value of the parameter α is required to be strictly bounded, $|\alpha| \leq 1$. Owing to smearing associated with the transverse momentum of the γ^*, predicted values of α are depressed below unity. For example,[15] $\alpha_t \simeq 0.8$.

Dynamical effects may also have a significant effect on the behavior of $d^2\sigma/d\cos\theta\, d\phi$. Higher order QCD gluonic radiation diagrams, such as shown in Fig.2, introduce interesting θ and ϕ dependences[16] which become more pronounced as $p_T(\gamma^*)$ increases. In $\pi^- N \to \gamma^* X$, high twist terms lead to the

expectation that $\alpha_t \to -1$ as $x_F \to +1$. High twist effects are discussed in more detail in Sec.V.

Data on $d\sigma/d\cos\theta\, d\phi$ seem to be of disappointing quality. A representative sample is shown in Fig.6. Fitted values of α fall in the range 0 to 1, but central values sometimes exceed unity and the quoted probable errors are large.[7,17,19,20] Good experimental acceptance at large $|\cos\theta|$ is obviously necessary for a good determination of α in Eq.(14). However, at large $|\cos\theta|$, one of the final leptons is slow in the laboratory, making both its detection and momentum measurement difficult.

Precise measurements of $d^2\sigma/d\cos\theta\, d\phi$ in different regions of x_F and p_T and for different values of $M/\sqrt{s}$ would provide valuable tests of both leading twist and higher twist terms in QCD. Analogous tests cannot be made readily in deep inelastic scattering. More experimental effort would seem very worthwhile.

III. FACTORIZATION

If we let $\sigma(M^2,x_F)$ denote the cross section for $AN \to \gamma^* X$, integrated over $p_T(\gamma^*)$, the factorization assumption states that we may write

$$M^4\sigma = \int \frac{dx_1}{x_1} \int \frac{dx_2}{x_2} \sum_{i,j} g_A^{(i)}(x_1,M^2) H_{i,j}(x_i,M^2) g_N^{(j)}(x_2,M^2) \ . \qquad (15)$$

I have omitted the usual delta functions which express various kinematic constraints.

In Eq.(15), the function $g_A^{(i)}$ depends only on hadron A and parton i; it is independent of the target N and of parton j. Likewise, $g_N^{(j)}$ depends only on N and j. The "hard scattering" cross section H_{ij} is independent of the hadrons A and N, and depends only on kinematic invariants associated with the hard subprocess $ij \to \gamma^* X'$.

As expressed above, Eq.(15) is the assertion of "weak factorization". Strong factorization adds the further requirement that the parton densities $g_A^{(i)}$ and $g_N^{(j)}$ are universal, process-independent functions measured, for example, in deep inelastic lepton scattering.

Factorization is a standard assumption in all applications of the parton model. Is it justified? Is it correct to assume that all "soft" hadronic effects can be absorbed into factorized probabilities g_A and g_N?

It has been known for many years that the proofs of factorization are incomplete.[3,21] In the language of perturbative QCD, initial state interactions via soft gluon exchanges are dangerous because these elementary gluons couple the partons from the two initial hadrons, "before" the pointlike annihilation occurs. Although these exchanges may take place over a long time scale, they should not affect the impulse approximation. The prediction of approximate scaling is unaffected. On the other hand, unless the effects of initial state interactions cancel order by order in perturbation theory, or after a sum is made to all orders, they complicate the possibility of relating parton densities to those measured in deep inelastic lepton scattering, they affect predictions of absolute yields, they imply potentially interesting nuclear A dependence of cross sections, and so forth.

Recently three groups have addressed the factorization issue in some detail, all within the context of perturbative QCD. Collins, Soper, and

Sterman[22] verify a weak form of factorization. Bodwin, Brodsky, and Lepage (BBL) claim that strong factorization fails in leading order.[23] Performing a calculation similar to that of BBL, Lindsay, Ross and Sachrajda (LRS) conclude that strong factorization is valid.[24] A subprocess typical of those considered is sketched in Fig.7. Gluons are exchanged between "active" constituents and between active and spectator constituents. BBL treat the full Glauber part of the active-active and active-spectator interactions (the longitudinal momenta of exchanged gluons are limited, $p_L^{c.m.} < m^2/\sqrt{s}$, where m is a typical hadronic scale). LRS examine active-spectator and active-active interactions involving the exchange of two gluons, without restricting the gluon longitudinal momenta. The apparent conflict between the conclusions of the two groups is a cause of concern, and the two groups are checking each other's calculations.

I will conclude this section with a brief discussion of some phenomenological implications.[23] If active-spectator interactions are important, one may expect a broadening of the p_T distribution when the γ^* is produced in a heavy nucleus.[25] The active constituent will scatter softly from $A^{1/3}$ spectators on its path through the nucleus, thereby gaining an increase in its transverse momentum. This increase is transmitted to the final γ^*. BBL estimate an increase in $\langle p_T^2(\gamma^*)\rangle \propto A^{1/3}(\Delta k_{T,col})^2$, where the increase per soft collision, $\Delta k_{T,col} \simeq 200$ MeV. Evidence in the data is mixed. For example, an indication of the expected increase may be found in the Columbia-Fermilab-Stony Brook data,[6] but the CERN NA3 group[26] observes no difference between $\langle p_T^2(\gamma^*)\rangle$ for $\pi^- p \to \gamma^* X$ and $\pi^- Pt \to \gamma^* X$. Note that $A^{1/3} \simeq 6$ for Pt. An independent examination of the effects of spectator interactions may be made in deep inelastic lepton scattering. The p_T distribution of final state

hadrons should be broader for production from nuclear targets. The European Muon Collaboration[27] examined data from experiments on Cu, C, and H_2 targets. No differences are observed out to $p_T \simeq 5$ GeV/c.

The absolute normalization of $d^2\sigma/dM^2dx_F$ may also be affected by active-spectator interactions.[23] Since the initial state interactions are soft, the longitudinal momentum specta of the initial partons are essentially unaffected. This means that the predicted M^2 and x_F dependences of $d^2\sigma/dM^2dx_F$ will not be altered. However, no matter how soft, the exchanged gluons carry color. The color of an active constituent may be changed by the soft processes, and the color factor of 1/3 included in Eq.(1) may have to be removed. A precise calculation of the new normalization factor is obviously difficult because it requires an integration which extends into regions of phase space where soft gluon propagators become singular. Estimates are discussed in Ref.23.

The factorization assumption is basic to all applications of the parton model in hadronic collisions, including

$$hN \to (\eta_c, J/\Psi, \chi, T, \ldots)X \; ; \tag{16a}$$

$$hN \to (\gamma, \pi, K, \ldots)X, \text{ at large } p_T \; ; \tag{16b}$$

and

$$hN \to \text{jets, charm, } \ldots \; . \tag{16c}$$

The process $hN \to \gamma^*X$ is simpler dynamically than all these others. It is the best "laboratory" for resolving the factorization question.

IV. ABSOLUTE YIELDS; K FACTORS

In the previous section I discussed the factorization issue, and I mentioned the corresponding uncertainties in theoretical predictions for the overall normalization of the yield of massive lepton pairs. In this section, I set the factorization question aside at the leading twist level. I revert to the assumption that the parton model, as improved by QCD, is valid for processes involving two hadrons in the initial state. I shall review the impact of higher order terms in the QCD $\log^{-1}(M^2/\Lambda^2)$ expansion on predictions for $d^2\sigma/dM^2dx_F$, especially its overall normalization. In Sec.II, I stated that the leading log contributions are all included when scale dependent parton densities are used, as in Eq.(6). In this section, we shall be concerned with the next-to-leading logarithms.

It has become popular to discuss normalization questions in terms of a "K-factor". This notation is unfortunate. The symbol K is often used to denote a constant, whereas the K factor may, and probably does depend on s, τ, and x_F. Second, on the theory side, the higher order dynamics which produces a factor $K > 1$ is distinct physics, by no means proportional to the physics of the annihilation term $q\bar{q} \to \gamma^*$.

A. Experiment

The experimental K factor is defined by

$$K_{exp}(s, \tau, x_F) = \frac{d^2\sigma_{exp}/dM^2dx_F}{d^2\sigma_{lead\ log}/dM^2dx_F} . \qquad (17)$$

The theoretical cross section in the denominator of Eq.(17) is that provided by the leading log annihilation model, Eq.(6). Although Eq.(17) is explicit enough, there are ambiguities in its application. For $pN \to \gamma^* X$, the required $q(x,M^2)$ and $\bar{q}(x,M^2)$ parton densities in the denominator must be obtained from an extrapolation outside the regions of x and $|Q^2|$ in which they are measured in deep inelastic lepton scattering. Moreover, the antiquark density $\bar{q}(x,M^2)$ is not well determined in deep inelastic scattering experiments. For example, non-trivial systematic uncertainty in $\bar{q}(x,Q^2)$ is associated with assumptions made about the ratio $R = \sigma_L/\sigma_T$. Sensitivity to these assumptions is particularly strong at small x, where the $\bar{q}(x,M^2)$ distribution is large.[5]

For all processes, $pN \to \gamma^* N$, $\bar{p}N \to \gamma^* N$, and $\pi N \to \gamma^* N$, uncertainty about the precise nuclear A dependence of cross sections affects knowledge of both the numerator and denominator of Eq.(17). For $\pi N \to \gamma^* N$, Eq.(17) cannot be used without further theoretical input since the distributions $q_\pi(x,M^2)$ and $\bar{q}_\pi(x,M^2)$ are "measured" only in lepton pair production. A normalization condition is usually imposed[9,19] whereby the valence part satisfies

$$\int_0^1 q_{\pi,v}(x,M^2)dx = 1 \ . \tag{18}$$

Although reasonable, Eq.(18) requires for its application that we make assumptions about the functional form of $q_{\pi,v}(x,M^2)$ at large x, and at small x, where it is not measured, as well as the assumption that $K_\pi(x,M^2)$ is independent of x, in disagreement with theoretical expectations. These systematic uncertainties on $K_{exp}^{\pi N}$ have not been discussed in the literature.

Table I: Compilation of $K_{exp}(\tau,x_F)$

Group	Beam and target	Momentum/$\sqrt{s}$ (GeV/c)/(GeV)	$K_{exp}(\tau,x_F)$ = Measured cross-section / Lead.Log. Drell-Yan prediction
NA3 Badier et al 1980	$(\bar{p}$ - p): Pt	150	2.3 ± 0.4
NA3 Badier et al 1979	p: Pt	200	2.2 ± 0.4
CFS Ito et al 1981	p: Pt	300/400	~1.7 $(2.5\pm)_{ELB}$
CHFMNP Antreasyan et al 1981	pp	44, 63	1.6 ± 0.2
MNTW Smith et al 1981	p: W	400	1.6 ± 0.3
A^2BCS Kourkoumelis et al 1981	pp	44, 63	~1.7
AFMcMS (E-537) Annassontzis et al 1982	$\bar{p}$: W, Cu, Be	125	2.25 ± 0.45
NA3 Lefrancois 1980	π^-: Pt	200	2.2 ± 0.3
NA3 Lefrancois 1980	π^+: Pt	200	2.4 ± 0.4
NA3 Lefrancois 1980	$(\pi^- - \pi^+)$: Pt	200	2.4 ± 0.4
AFMcMS (E-537) Annassontzis et al 1982	π^-: W, Cu, Be	125	2.5 ± 0.5

A compilation of data[6-9,17,19,28] on $K_{exp}(s,\tau,x_F)$ is presented in Table I. Different τ and x_F intervals are spanned by the different experiments. The values of K listed in the table are those quoted in the experimental papers. The quoted probable errors in most cases do not include estimates of the systematic uncertainties discussed above, nor other systematic uncertainties in the deep-inelastic lepton data from which the parton densities are extracted. Different sets of parton densities are employed by the different experimental groups listed in the table. In some cases, the densities employed to evaluate the denominator of Eq.(17) are structure functions appropriate at some average M^2 of the experiment in question, but M^2 dependence is not included.

The expression

$$K_{exp} \simeq 2.0 \pm 0.6 \tag{19}$$

provides a very rough summary of present data. Dependences of K_{exp} on τ, on x_F, and on the type of beam particle are not excluded but are not established. When data were available only from $pN \to \gamma^*X$, it was tempting to suggest[2] that different ocean quark densities are probed in DIS and in massive lepton pair production, with $\bar{q}_p(DY) \simeq 2\bar{q}_p(DIS)$. I am still intrigued by this possibility. However, the data in Table I show that the same value $K_{exp} \simeq 2$ is consistent with data from both valence dominated processes, such as $\pi^-N \to \gamma^*X$ and $\bar{p}N \to \gamma^*N$, and valence-sea processes, $pN \to \gamma^*X$. To obtain the estimate quoted in Eq.(19) for the uncertainty in K_{exp}, I used the Columbia-Fermilab-Stony Brook data[6] on $pN \to \gamma^*X$ and computed K_{exp} for two different choices of parton densities, the 1979 q and $\bar{q}$ densities[29] of the CERN-Dortmund-

Heidelberg-Saclay $\nu,\bar{\nu}$ Collaboration (CDHS), and the 1982 q and $\bar{q}$ densities also reported by CDHS.[5] I obtain K_{exp}('79 densities) ≈ 1.7, and K_{exp}('82 densities) ≈ 2.5. The substantial change of K_{exp} from 1.7 to 2.5 is due to improved knowledge of the deep inelastic parton densities $q(x,M^2)$ and $\bar{q}(x,M^2)$.

B. Theory

Some of the QCD subprocesses which contribute to γ^* production are sketched in Fig.2. The contributions of all processes to $d^2\sigma/dM^2dx_F$ through first order in α_s have been computed by several groups.[30-32] For each flavor f, they obtain

$$\frac{1}{\sigma_0}\frac{d\sigma}{dM^2} = \int\int \frac{dx_1}{x_1}\frac{dx_2}{x_2}\left[q(x_1,M^2)\bar{q}(x_2,M^2) + (1\leftrightarrow 2)\right]\delta(1-z)$$

$$+ \int\int \frac{dx_1}{x_1}\frac{dx_2}{x_2}\left[q(x_1,M^2)\bar{q}(x_2,M^2) + (1\leftrightarrow 2)\right] \times$$

$$\frac{\alpha_s(M^2)}{2\pi}\left[\frac{4}{3}\pi^2\delta(1-z) + \bar{f}_{q\bar{q}}(z)\right] \qquad (20)$$

$$+ \int\int \frac{dx_1}{x_1}\frac{dx_2}{x_2}\left[\left(q(x_1,M^2) + \bar{q}(x_1,M^2)\right)G(x_2,M^2) + (1\leftrightarrow 2)\right] \times$$

$$\frac{\alpha_s(M^2)}{2\pi} f_{qG}(z) \ .$$

Here $z = M^2/(x_1x_2s)$, and $\sigma_0 = 4\pi\alpha^2e_f^2/(9sM^2)$. I will not specify the functions $\bar{f}_{q\bar{q}}(z)$ and $f_{qG}(z)$. The first term in Eq.(20) is the standard annihilation model prediction, with scale dependent structure functions. It is the full leading log result. The next two terms are next-to-leading log contributions; they are proportional to $\alpha_s(M^2) \propto 1/\ell n\ M^2$. In Eq.(20), $G(x,M^2)$ denotes the

gluon structure function.

Together, the two next-to-leading log contributions in Eq.(20) are roughly equal in numerical value to the leading log piece. We may define a theoretical K factor, $K_{th}^{O(\alpha_s)}(s,\tau,x_F)$, by dividing Eq.(20) by the leading log result (i.e. divide Eq.(20) by the first term on the right hand side). A numerical evaluation[31] of $K_{th}^{O(\alpha_s)}$ is presented in Fig.8. For both $pN \to \gamma^*X$ and $\pi^-N \to \gamma^*X$, $K_{th}^{O(\alpha_s)}(\tau)$ is in the range 1.8 to 2.0 for $0.02 < \tau < 0.4$. the x_F dependence of $K_{th}^{O(\alpha_s)}(\tau,x_F)$ is discussed in Ref.32. To my knowledge, a full computation of K_{th} through order α_s^2 has not yet been completed. The $O(\alpha_s^2)$ result will involve contributions from qq scattering and is expected to influence the behavior of K strongly at large x_F.

At least implicitly, the experimental K_{exp} involves a sum to all orders in α_s, whereas K_{th} is computed only through first order. Nevertheless, it is tempting to compare the values of the two, especially since both are in the neighborhood of K = 2.0, and tempting to suggest that QCD predicts the normalization dicrepancy discussed above, $K_{exp} \simeq 2$. The fact that $K_{th}^{O(\alpha_s)}(\tau,x_F)$ is roughly independent of τ and x_F in the ranges explored experimentally [$0.15 < \tau^{1/2} < 0.5$, and x_F small], may also explain why the leading log annihilation model provides the correct shapes in M^2 and x_F of $d^2\sigma/dM^2dx_F$. Likewise, the fact that $K_{th}(\tau,x_F)$ rises rapidly as $x_F \to 1$ suggests that care is in order when data on $\pi^-N \to \gamma^*X$ are interpreted. In particular, the data provide the product $K(x)q_\pi(x,M^2)$, not $q_\pi(x,M^2)$. If $K(x) \sim (1-x)^{-1}$, then data imply $q_\pi(x,M^2) \sim (1-x)^2$.

The decomposition of K_{th} in Fig.8 indicates that the quark-gluon term, the third term in Eq.(20), is relatively unimportant. For $M/\sqrt{s} \lesssim 0.45$, the dominant contribution to $K_{th}^{O(\alpha_s)}$ is provided by the terms proportional

to $\delta(1-z)$ on the right-hand-side of Eq.(20). Therefore, through $O(\alpha_s)$, Eq.(20) may be reexpressed as

$$\frac{d^2\sigma}{dM^2} = \frac{d^2\sigma_{\text{lead log}}}{dM^2}\left[1 + \frac{\alpha_s}{2\pi}\frac{4}{3}\pi^2\right] + \alpha_s\{\ldots\} , \tag{21}$$

where the term $\{\ldots\}$ is relatively unimportant for $M/\sqrt{s} \lesssim 0.45$. For a typical $\alpha_s = 0.3$,

$$\left[1 + \frac{\alpha_s}{2\pi}\frac{4}{3}\pi^2\right] = 1.63 . \tag{22}$$

Troubling questions about the convergence of the perturbation expansion are raised by the fact that the $O(\alpha_s)$ term in the asymptotic series, Eq.(22), provides a 63% correction. Important work is being done to identify the source of the large correction.[33,34] It is known[31] that the term $4\pi^2/3$ in Eq.(21) arises from an analytic continuation of the $O(g^2)$ gluon vertex correction amplitude from $Q^2 < 0$, in deep inelastic lepton scattering, to $Q^2 > 0$ appropriate for massive lepton pair production:

$$\begin{aligned} A_{DIS} &= C_F \frac{\alpha_s}{2\pi} \ell n^2 Q^2 ; \\ A_{DY} &= C_F \frac{\alpha_s}{2\pi} \ell n^2(-Q^2) ; \\ \text{Re}[A_{DY} - A_{DIS}] &= \frac{\alpha_s}{2\pi}\pi^2 C_F . \end{aligned} \tag{23}$$

Here $C_F = 4/3$. At each order n in perturbation theory, such $\log^{2n}Q^2$ terms from gluon vertex corrections should yield π^2 terms having the form

$$C_F^n \left(\frac{\alpha_s}{2\pi}\right)^n \frac{\pi^{2n}}{n!} .$$

This result suggests that the π^2 terms may be exponentiated, and that we should find

$$\frac{d\sigma}{dM^2} = \exp\left[\frac{\alpha_s}{2\pi}\frac{4}{3}\pi^2\right]\frac{d\tilde{\sigma}}{dM^2} . \tag{24}$$

The task becomes one of demonstrating that $d\tilde{\sigma}/dM^2$ has better convergence properties than $d\sigma/dM^2$. To verify this, complete computations must be done through at least $O(\alpha_s^2)$.

Even if the large higher order π^2 contributions to $K_{th}(s,\tau,x_F)$ can be summed, we may note that the $\frac{4}{3}\pi^2\alpha_s(M^2)$ term on the right hand side of Eq.(20) is only part of the next-to-leading log contribution. Figure 8 indicates that at large τ the $\bar{f}_{q\bar{q}}(z)$ contribution becomes the dominant contribution to K_{th} in $O(\alpha_s)$. It is unclear whether simple statements can be made about the expected convergence properties of K_{th} for $x_F \to 1$ or for $\tau \to 1$.

It is curious that the leading log QCD effects, scaling violations, are essentially unobservable in $hN \to \gamma^* X$, but that the next-to-leading order effects are large. In order $O(\alpha_s)$, they appear to be large enough to account for the observed $K_{exp} \simeq 2$. On the other hand, such large effects raise doubts about the reliability of the theoretical expansion. Can theory aspire to better accuracy than ±30% on K? Experimentally, it is surely important to pin down the size of $K_{exp}(\tau,x_F)$ and its dependence on τ and x_F. Present uncertainties in the data do not challenge QCD. The task requires better measurements of nuclear A dependence in both $hN \to \gamma^* X$ and in deep inelastic

scattering, as well as control of systematic uncertainties in our knowledge of $\bar{q}(x,Q^2)$ from DIS. High statistics antiproton experiments would permit the best determination of $K_{exp}(\tau,x_F)$ since the leading log theoretical predictions for $\bar{p}p \to \gamma^*X$ are governed by $F_2(x,Q^2)$, which is well determined experimentally in the relevant ranges of x and Q^2.

V. HIGH TWIST

In the usual leading twist approximation of the QCD improved parton model, the quark structure function of the nucleon is expected to behave at large x as

$$q(x,Q^2) \to (1-x)^{3+c\ell n\ell nQ^2} \quad . \tag{25}$$

The structure function $F_2(x,Q^2)$ will behave likewise. However, competing terms may become important at small enough (1-x). These competing inverse-power high-twist terms behave at small (1-x) as $(1-x)^2/Q^2$, $(1-x)/Q^2$, and so forth. They are associated with hard momentum sharing between more than one active parton in a given hadron. Their magnitude is determined by typical hadronic scales, ~1 GeV. In analyses of deep inelastic scattering data, it is difficult to separate the high-twist inverse-power contributions in Q^2 from the more familiar gluonic radiation $\ell n\ Q^2$ effects.[5] An extra handle on the high-twist pieces is obviously desirable. In purely inclusive deep inelastic scattering, the ratio σ_L/σ_T provides such a filter, but the measurement is difficult.[35]

It has been argued that $\pi^-N \to \gamma^*X$ is especially useful for isolating and

studying high twist dynamics.[36] The leading twist term in the pion structure function is predicted to behave at large x as $q_\pi(x) \to (1-x)^2$, with $\ell n\, \ell n\, Q^2$ modification. The high-twist contribution adds a term which is independent of x. As $x \to 1$,

$$q_\pi(x,M^2) \to (1-x)^2 + \frac{\lambda^2}{M^2} . \tag{26}$$

This implies that the high-twist term should dominate in $\pi^- N \to \gamma^* X$ at large x_F. Second, the high twist term produces a massive photon with longitudinal helicity, yielding an angular distribution $d\sigma/d\cos\theta \propto \sin^2\theta$ in the massive photon rest frame.[36] This prediction contrasts with the usual leading twist expectation of transverse polarization, and $d\sigma/d\cos\theta \propto (1 + \cos^2\theta)$.

Theory and data are compared in Fig.9. The coefficient α in the expression $d\sigma/d\cos\theta = (1 + \alpha\cos^2\theta)$ is predicted to decrease from $\alpha \cong +1$ to $\alpha = -1$ as $x_F \to 1$. The Chicago-Illinois-Princeton data[37] at 225 GeV/c confirm this expectation, but subsequent data from the CERN NA3 collaboration[38] disagree. Poor experimental acceptance in the $\cos\theta$ distribution near $\cos\theta = \pm 1$ undermines confidence in the experimental results. A new experiment[39] designed with excellent experimental acceptance over the full range of θ and ϕ will soon yield definitive data on the x_F dependence of angular distributions.

The magnitude of λ^2 in Eq.(26) is predicted.[36] The high twist diagram which produces the $\sin^2\theta$ effect in $\pi N \to \gamma^* X$ also leads to very interesting phenomena in other reactions, including $\nu N \to \mu^- \pi X$, $\gamma N \to \pi X$ at large p_T, and $\pi N \to \gamma X$ at large p_T. Some of these related processes are discussed in Refs.36 and 40.

VI. TRANSVERSE MOMENTUM DISTRIBUTIONS AND SOFT GLUONS

I summarized data on the energy dependence of the moments $\langle p_T^2 \rangle$ and $\langle p_T \rangle$ in Sec.II.F, and I mentioned that the growth of $\langle p_T^2 \rangle$ with s is evidence for an underlying quantum field theory of the strong interactions. In QCD, which has no intrinsic scale, and which has a dimensionless coupling strength, one expects[2]

$$\langle p_T^2 \rangle = s\alpha_s("Q^2")F(\tau,x_F,\alpha_s) + (\ldots) \ . \tag{27}$$

The term (...) denotes contributions which do not grow with s, including, for example, high twist terms and parton intrinsic k_T effects. It is not a simple matter to specify the scale "Q^2" at which α_s in Eq.(27) is evaluated. The size and functional form of $F(\tau,x_F)$ in Eq.(27) are determined by (a) structure functions; (b) hard parton cross sections for the $O(\alpha_s)$ QCD subprocesses $qG \to \gamma^* q$ and $q\bar{q} \to \gamma^* G$ which supply the large p_T of the γ^*; and (c) higher order "$K'(p_T)$" factors associated with $O(\alpha_s^2)$ and beyond. The theoretical uncertainties in predicting the slope $b = \alpha_s("Q^2")F(\tau,x_F,\alpha_s)$ are at the level of a factor of 2 or 3. Nevertheless, the $O(\alpha_s)$ QCD predictions I made for b in 1978 are not in grose disagreement with data. A figure from my Vanderbilt conference talk[2] is reproduced here, Fig.10. At $M/\sqrt{s} = 0.22$, my curve yields $b_{th} = 1.1 \times 10^{-3}$ GeV^{-2} to be compared with $b_{exp} = (1.4 \pm 0.2) \times 10^{-3}$ GeV^{-2} in Eq.(12). Presumably the incorporation of $O(\alpha_s^2)$ contributions would improve agreement of theory and experiment.

A. Extrapolations to Collider Energies.

The empirical fit provided in Fig.5 may be extrapolated to the center-of-mass energy of the CERN $S\bar{p}pS$ collider, $\sqrt{s} = 540$ GeV. One finds $\langle p_T \rangle \simeq 14$ GeV at mass $M = 120$ GeV which is not too far above the expected mass of the $W^{\pm}$ and Z°. This extrapolation of the data agrees with the estimate[2] I made in 1978. It suggests that the $W^{\pm}$ and Z° will be produced with non-trivial $\langle p_T \rangle$ at the $S\bar{p}pS$ and be accompanied by substantial recoil hadron energy. A few notes of caution are in order concerning the reliability of this "prediction". The data used in the extrapolation are pN data not $\bar{p}p$ data. Purely $O(\alpha_s)$ QCD calculations indicate[2] that somewhat larger values of the slope b, Eq.(10), are expected for $\bar{p}N$ relative to pN. I do not know what influence $O(\alpha_s^2)$ "corrections" have on the difference of the slopes $(b_{\bar{p}N} - b_{pN})$. Second, $O(\alpha_s)$ calculations[2] (and limited data) show that the slope b decreases strongly as $M/\sqrt{s}$ is decreased from ~ 0.2 to zero (see Fig.10). This effect would tend to reduce estimates of $\langle p_T \rangle$ of the Z° and $W^{\pm}$. Third, both the fits and my calculations ignore possible logarithmic effects; e.g. the slope b may be proportional to $\ell n^{-1}(M^2/\Lambda^2)$. In summary, at the $S\bar{p}pS$ collider, the $W^{\pm}$ and the Z° are expected to be produced with $\langle p_T \rangle$ in the range 10 to 20 GeV/c.

At the Fermilab collider, $\sqrt{s} = 2$ TeV, the $W^{\pm}$ and Z° masses correspond to $M/\sqrt{s} \simeq 0.04$. Arguments mentioned above suggest that the slope, b, should be substantially less[2] at $M/\sqrt{s} \simeq 0.04$ than that measured at $M/\sqrt{s} \simeq 0.22$. For an assumed mass of 90 GeV for the Z°, my computations lead to the following expectations:

$\sqrt{s}$	$M/\sqrt{s}$	Predicted Slope, b	$\langle p_T^2 \rangle_Z$	$\langle p_T^2 \rangle_Z^{1/2}$
800 GeV	0.11	0.78 GeV^{-2}	499 GeV^2	22 GeV
2000 GeV	0.045	0.35 GeV^{-2}	1400 GeV^2	37 GeV

The root-mean-square value, $\langle p_T^2 \rangle_Z^{1/2}$, is probably an overestimate of the true mean $\langle p_T \rangle$. A possible logarithmic factor in b is another effect which may depress $\langle p_T \rangle$. On the other hand, my predicted slope b is somewhat too small, as I indicated above. Putting all these uncertainties together, I hazard the conservative estimate that $\langle p_T \rangle \simeq 25$ to 35 GeV/c for Z° and $W^\pm$ production at $\sqrt{s}$ = 2 TeV.

The extrapolations discussed above are appropriate for $x_F \simeq 0$. Data[41] at current fixed target energies ($\sqrt{s} < 30$ GeV) indicate little change of $\langle p_T \rangle$ with x_F. First order QCD would prefer a decrease[2], especially dramatic for $|x_F| \gtrsim 0.5$. At low energies, there are at least two important contributions to the size and kinematic dependence of $\langle p_T \rangle$: the intrinsic and high-twist effects which supply the intercept, a, in Eq.(10), and the QCD hard scattering effects which supply the slope b. Since the x_F dependence of the two effects has not been disentangled at $\sqrt{s} < 30$ GeV, it is difficult to make reliable estimates of the x_F dependence of $\langle p_T \rangle$ at collider energies.

B. Cross Sections as a Function of p_T.

Data on the p_T dependence of $d^3\sigma/dM^2 dx_F p_T^2$ extend to $p_T \simeq 5$ GeV/c in π^-N, pN, and pp interactions.[6,26] An example is presented in Fig.11. These data[26] show that the large p_T tail ($p_T \gtrsim 2$ GeV/c) fans out as s is increased, consistent with QCD expectations. However, the scaling expected theoretically at large p_T,

$$\frac{d^3\sigma}{dM^2 dy dp_T^2} = \frac{1}{s^2 p_T^2} H(x_T, \tau, y) \ , \tag{28}$$

has not yet been verified. Here $x_T = 2p_T/\sqrt{s}$. Data are expected soon at larger values of p_T from three experiments in progress: π^-N, CERN-Ecole Polytechnique-Strasbourg-Zurich, NA-10; π^-N, Chicago-Princeton, E-326; and pN, Columbia-Fermilab-Stony Brook-Univ. of Washington-KEK-Kyoto-Saclay-CERN, E-605.

In first order QCD, the transverse momentum of the massive photon is produced by the $q\bar{q} \to \gamma^* G$ and $qG \to \gamma^* q$ subprocesses illustrated in Fig.2. The $q\bar{q} \to \gamma^* G$ subprocess is dominant[2] in $\pi^- N \to \gamma^* X$ and in $\bar{p}N \to \gamma^* X$, implying that the γ^* is balanced in p_T by a gluon jet in these two reactions. In $pN \to \gamma^* X$, the $qG \to q\gamma^*$ subprocess is prevalent[2], meaning that a recoil quark jet balances the p_T of the γ^*. Note that the γ^* is itself a clean unambiguous "jet".

Many subprocesses contribute to the p_T distribution in second order, $O(\alpha_s^2)$. A few of these are sketched in Fig.2(f)-2(h). In some, a quark or a gluon jet emerges in the same region of phase space as the γ^*. Correspondingly, a study of the distribution of hadronic energy in association with a γ^* at large p_T may provide limits on the relative importance of $O(\alpha_s^2)$ and higher subprocesses.[42]

Ellis, Martinelli, and Petronzio[43] have computed the $O(\alpha_s^2)$ contributions to the distribution $d\sigma/dp_T^2$. They consider only the difference of the cross sections for $\pi^- N \to \gamma^* X$ and $\pi^+ N \to \gamma^* X$. In this difference all subprocesses involving initial gluons are eliminated. Their results may be expressed in terms of a factor $K'_{th}(p_T)$,

$$K'_{th}(p_T) = \frac{\frac{d\sigma}{dp_T^2}\left[O(\alpha_s) + O(\alpha_s^2)\right]}{\frac{d\sigma}{dp_T^2}\left[O(\alpha_s)\right]} , \tag{29}$$

which represents the importance of $O(\alpha_s^2)$ contributions relative to $O(\alpha_s)$. Inclusion of $O(\alpha_s^2)$ contributions approximately doubles the predicted cross section in the range $2.0 < p_T < 4.0$ GeV/c. The relative effect is larger when final results are convoluted with a Gaussian distribution selected to represent the non-perturbative intrinsic k_T spectra of the initial partons.[43] As will be noted, the numerical value of K'_{th} is roughly equal to that of $K_{th}(\tau,x_F)$ discussed earlier, in Sec.IV. However, the underlying dynamics are different in the two cases. There is no "universality" behind the approximate equalities $K'_{th} \simeq K_{th} \simeq 2$.

Turning to a direct comparison of theoretical and experimental distributions, I begin with results[2] shown in Fig.12. These $O(\alpha_s)$ results illustrate the serious problems which must be addressed if QCD computations are to be extended to describe the relatively small values of p_T ($p_T \lesssim 2$ GeV/c) where the experimental cross section is large. In the computations for which results are shown in Fig.12, the partons are assumed to be massless, and no intrinsic k_T effects are included. After $O(\alpha_s^2)$ contributions are incorporated $\left(K'(p_T) \simeq 2\right)$, theory would probably agree[44] with data fairly well at large p_T ($\gtrsim 3$ GeV/c). The p_T^{-2} divergence of the theoretical results as $p_T \to 0$ may be removed if off-shell initial parton kinematics are employed.[45] A simple procedure for including intrinsic k_T effects, devised by Altarelli, Parisi, and Petronzio,[46] is often employed to

transform the disagreement apparent in Fig.12 into a "perfect" fit to data. Although not inconsistent with QCD such procedures are primarily cosmetic, and it is generally agreed that they do not test the theory in a meaningful way.

The essential problem is that the $O(\alpha_s)$ and $O(\alpha_s^2)$ QCD computations apply only when $p_T \sim M \sim \sqrt{s}$, i.e., where there is only one large momentum scale. Data tend to be confined to much smaller values of p_T. Recognizing this difficulty, several groups are addressing the problem of providing a predictive QCD description of processes in which there are two different momentum scales.[47-49] The goal is to specify properties of the distribution $d\sigma/dp_T^2$ in the region

$$\Lambda \ll p_T \ll cM \ , \tag{30}$$

where c is constant. Although it is doubtful that current data fall within the limits indicated in Eq.(30), the theoretical results should be valuable when data are extended to larger values of p_T and M.

A considerable increase in theoretical complexity is involved in treating the region defined by (30). In addition to large logarithmic contibutions proportional to $\ell n(M^2/\Lambda^2)$, terms proportional to powers of $\ell n(M^2/p_T^2)$ must also be summed. At fixed M^2, the cross section $d\sigma/dp_T^2$ receives contributions from a series of terms having the appearance

$$\frac{1}{p_T^2 M^2}\left[1 + a_1\alpha_s \ell n^2(M^2/p_T^2) + O(\alpha_s^2 \ell n^4) + \ldots \right.$$
$$\left. + b_1\alpha_s \ell n\,(M^2/p_T^2) + O(\alpha_s^2 \ell n^2) + \ldots\right] . \tag{31}$$

These terms correspond to physical processes in which an active constituent radiates soft gluons before the hard annihilation $q\bar{q} \to \gamma^*$. The chain of soft gluon emissions is responsible for evolution of the structure functions, $\bar{q}(x,\Lambda^2) \to \bar{q}(x,M^2)$; it generates a dynamical component to the parton "intrinsic" k_T distribution; it provides an increase in transverse energy and associated hadronic multiplicity, related to M^2; and, of interest here, damps the p_T^{-2} divergence of the $O(\alpha_s)$ QCD computation in the small p_T region.

When the leading $\alpha_s^n \log^{2n}(M^2/p_T^2)$ contributions in (31) are summed, one obtains

$$\frac{d^2\sigma}{dM^2 dp_T^2} \propto \frac{K'(p_T)\alpha_s}{M^2 p_T^2} \exp\left[-\frac{\alpha_s}{2\pi}\left(\frac{4}{3}\right)\ell n^2\left(\frac{M^2}{p_T^2}\right)\right] . \tag{32}$$

The first factor on the right-hand-side of Eq.(32) is the $O(\alpha_s)$ QCD result, multiplied by the factor $K'(p_T)$ discussed above. The second, exponential, factor is a Sudakov form factor associated with soft gluon radiation. It vanishes as $p_T \to 0$, manifesting the fact that the probability is zero for the emission of no gluons (and thus no p_T). When less restrictive approximations are used in the calculations, the soft gluon "correction" factor vanishes less rapidly than that shown in Eq.(32). For example, $p_T(\gamma^*) = 0$ may arise from a configuration in which two hard gluons are emitted with $\vec{k}_{T1} = -\vec{k}_{T2}$.

The cross section in Eq.(32) decreases both as $p_T^2 \to M^2$ and as $p_T^2 \to 0$. There is a peak in the distribution between these two limits. Equation (32) is known not to be reliable at small p_T since all next-to-leading log terms become equally important in this limit. Systematic analytic and numerical methods are being developed to handle necessary summations, in momentum and in impact parameter spaces.[47-51] It is unclear whether these calculations can be

improved to the point of providing reliable, quantitative predictions for $d\sigma/dp_T^2$ in the "small" p_T region, $p_T < 2$ GeV. Many delicate approximations are associated with how kinematic constraints are handled, with orderings of the gluon transverse momenta, with neglect of inverse power contributions, and so forth.

In practice, impressive fits to data are obtained when the soft gluon Sudakov effects are included. An example[50] is presented in Fig.13. Ad-hoc parton intrinsic k_T distributions must still be incorporated, but the fitted values of $\langle k_T \rangle$ turn out to be somewhat smaller. One should ask, of course, how much of the perfect fit to data is due to perturbative QCD, how much is due to gluon Sudakov effects, and how much is put in "by hand" as an intrinsic k_T distribution.

Questions may be addressed in three different regions of p_T. In the large p_T region ($p_T \gtrsim 3$ GeV/c?), checks of scaling are important, as are comparisons of absolute yields with $O(\alpha_s)$ and $O(\alpha_s^2)$ QCD predictions. Second, at somewhat smaller values of p_T, one enters the domain of soft gluon radiation effects. Here it is important to check the expected broadening of the p_T distribution as M is increased, at fixed $M/\sqrt{s}$ and x_F. This point has been emphasized by Collins and Soper.[47,51] Third, there is the small p_T ($\lesssim 2$ GeV/c?) region dominated by parton intrinsic k_T distributions. Measurements should provide relevant information on the x dependence of these k_T spectra, not calculable in perturbative QCD, perhaps, but at least approximately calculable in models of hadronic structure, including lattice gauge theory simulations and bag models. It would be interesting to establish whether important differences exist in the experimental energy dependence (scaling properties) of the distribution $d^3\sigma/dM^2dx_Fdp_T^2$ at large and small p_T.

VII. L'ENVOI

More could be written on several items not treated in this report, including electroweak asymmetries, spin-polarization effects, Higgs phenomena, the expected properties of the "jets" of associated hadrons (beam, target, and high p_T recoil jets), the emergence of a plateau in the rapidity spectrum of associated hadrons, and predictions for the growth with Q^2 of associated multiplicities. I will comment on only one of these items: polarization. In both the classical and the QCD leading log versions, the $\bar{q}q$ annihilation model requires the helicities of the q and $\bar{q}$ to be opposite, and the asymmetry $\hat{A}_{LL}$ at the constituent level is predicted: $\hat{A}_{LL} = -1$. Here, $\hat{A}_{LL} = (\hat{\sigma}_{++} - \hat{\sigma}_{+-})/(\hat{\sigma}_{++} + \hat{\sigma}_{+-})$. Because the dominant contribution to $hh \to \gamma^* X$ at the next-to-leading log level is of the form $\alpha_s(M^2)\,\frac{4}{3}\,\pi^2\,\bar{q}(x_1,Q^2)q(x_2,Q^2)$, i.e. proportional to $\bar{q}q$, the prediction $\hat{A}_{LL} = -1$ is preserved even when the large next-to-leading log effects are included. Measurements of $\hat{A}_{LL}$ would therefore be an especially valuable check on the basic applicability of the annihilation mechanism and higher-order QCD corrections to it. My enthusiasm is tempered by two problems. First, the measurement requires longitudinally polarized antiquarks as well as quarks. I do not know whether the sea in a proton can be polarized. Polarized valence antiquarks in an antiproton would be a solution to this difficulty, but I doubt that intense sources of high energy polarized antiprotons will be available soon. If experiments can be done, and $\hat{A}_{LL} = -1$ is verified for the Drell-Yan continuum, then observed deviations from $\hat{A}_{LL} = -1$ as one scans through the range of values of M should provide useful insight into mechanisms for the hadronic production of J/Ψ, Υ

and other resonances for which the continuum is just a "background".

In this report I have focused primarily on recent experimental and theoretical investigations. As I discussed in Sec.III, the parton model factorization assumption is being scrutinized by at least three groups. It is not clear whether perturbative QCD justifies this aspect of the model. Some phenomenological implications of the breakdown of factorization were also reviewed.

If the validity of factorization is assumed, then QCD justifies the annihilation model as the correct leading-log QCD model for lepton pair production. However, the next-to-leading log terms are large. Through first order in α_s, their contribution nearly doubles the predicted yields. While this increase is welcome from the standpoint of data, the large $O(\alpha_s)$ "correction" raises doubts about the convergence of the perturbation series. Large higher order terms are found in theoretical analyses of other processes also, but only, to my knowledge, where data seem to require them. A systematic understanding is obviously called for.[52] Precise data on the size and kinematic variation of $K_{exp}(\tau,x_F)$ is desirable.

High-twist terms, with their inverse power dependence on the large momentum variable Q^2 are potentially important and must be included in quantitative analyses of all hard scattering processes. The experimental study of the behavior of the decay angular distributions in the γ^* rest frame in $\pi^-N \to \gamma^*X$ at large x_F should establish the size of a particular, calculable high twist term.[36,40]

In concluding my discussion of transverse momentum spectra in Sec.VI, I defined three different regions of $p_T(\gamma^*)$ and listed questions of interest for each. Considerable progress has been made in attempts to sum soft gluon

effects, but more work must be done to establish a quantitative phenomenology of p_T spectra at modest values of p_T.

In many respects, $hN \to \gamma^* X$ is the "best hard scattering process", both theoretically and experimentally, for resolving many of the questions discussed in this report. The questions are basic to the application of QCD to all other hadron-hadron hard scattering processes, as well as to hadronic final states in deep inelastic lepton scattering and electron positron annihilation.

REFERENCES

1. More information on many theoretical and experimental topics may be found in the Moriond Workshop on Lepton Pair Production, Les Arcs, 1981 (Paris: Editions Frontieres, 1981) Ed. by J. Tran Thanh Van. See also L. Lederman, Proc. XIX Int. Conf. on High Energy Physics, Tokyo, 1978; J. Pilcher, Proc. 1979 Int. Symp. on Lepton and Photon Interactions at High Energies, Fermilab, 1979, R. Stroynowski, Phys. Rep. C71, 1 (1981), and I. Kenyon, CERN report CERN-EP/82-81 (1982), to be published in Reports on Progress in Physics.
2. E. L. Berger, Proc. 3rd Int. Conf. at Vanderbilt Univ. on New Results in High Energy Physics, 1978; (New York: AIP Conf. Proc. No.45); E. L. Berger, Proc. 1978 Int. Meeting on Frontier of Physics, Singapore (Singapore: National Academy of Sciences, 1978); E. L. Berger, High Energy Physics in the Einstein Centennial Year, Orbis Scientiae, 1979 (N.Y.: Plenum Press, 1979).

3. S. D. Drell and T.-M. Yan, Phys. Rev Letters 25, 316 (1970), and Ann. Phys. 66, 578 (1971); S. D. Drell, these proceedings.

4. H. D. Politzer, Nucl. Phys. B129, 301 (1977); C. T. Sachrajda, Phys. Lett. 73B, 185 (1978); D. Amati, R. Petronzio, and G. Veneziano, Nucl. Phys. B140, 54 (1978); R. K. Ellis, H. Georgi, M. Machacek, H. D. Politzer, and G. Ross, Nucl. Phys. B152, 285 (1979); A. Mueller, Phys. Rev. D9, 963 (1974).

5. CERN-Dortmund-Heidelberg-Saclay collaboration, F. Eisele, XXI International Conference on High Energy Physics, Paris, 1982.

6. Columbia-Fermilab-Stony Brook collaboration, A. S. Ito et. al., Phys. Rev. D23, 604 (1981).

7. CERN-Harvard-Frascati-MIT-Naples-Pisa collaboration, D. Antreasyan et. al., MIT report 119 (1981) and Phys. Rev. Lett. 45, 863 (1980).

8. Fermilab-Athens-McGill-Michigan-Shandong (E-537) collaboration, E. Anassontzis et. al., Fermilab report CONF-82/50-EXP submitted to XXI Int. Conf. on High Energy Physics, Paris, 1982; B. Cox, these proceedings.

9. Saclay-CERN-College de France-Ecole Polytechnique-Orsay (NA3) collaboration, L. Lefrancois, Proc. XX Int. Conf. on High Energy Physics, Madison, 1980 (New York: AIP Conf. Proc. No.68).

10. A. Mueller, Columbia Univ. report CU-TP-232, XVII Rencontre de Moriond (1982); A. Mueller, these proceedings. J. D. Bjorken, private communications.

11. European Muon Collaboration, J. J. Aubert et. al. XXI Int. Conf. on High Energy Physics, Paris, 1982.

12. I. R. Kenyon, CERN report CERN-EP/82-81 (1982), to be published in Reports on Progress in Physics.

13. P. K. Malhotra, these proceedings.

14. J. Collins and D. Soper, Phys. Rev. D16, 2218 (1977); J. Collins, Phys. Rev. Lett. 42, 291 (1979).

15. E. L. Berger, J. Donohue, and S. Wolfram, Phys. Rev. D17, 858 (1978).

16. R. J. Oakes, Nuovo Cimento 44, 440 (1966); E. L. Berger, Zeit. Phys. C4, 289 (1980); J. Donohue in Phenomenology of Quantum Chromodynamics, Rencontre de Moriond, 1978, Vol.I. p.159; K. Kajantie, J. Lindfors, and R. Raitio, Phys. Lett. 74B, 384 (1978); C. S. Lam and W.-K. Tung, Phys. Rev. D18, 2447 (1978) and Phys. Lett. 80B, 228 (1979) and Phys. Rev. D21, 2712 (1980); P. W. Johnson and W.-K. Tung, Phys. Rev. Lett. 45, 1382 (1980); J. Cleymans and M. Kuroda, Bielefeld report BI-TP 81/16 (1981); R. L. Thews, Phys. Rev. Lett. 43, 987 (1979).

17. Athens-Athens-Brookhaven-CERN-Syracuse collaboration, C. Kourkoumelis et. al., Phys. Lett. 91B, 475 (1980) and Moriond Workshop on Lepton Pair Production, p.125.

18. CERN-Columbia-Oxford-Rockefeller collaboration, A.L.S. Angelis et. al., Phys. Lett. 87B, 398 (1979) and paper contributed to the Int. Symp. on Lepton and Photon Interactions, Batavia, Illinois.

19. CERN NA3 collaboration, J. Badier et. al., Phys. Lett. 89B, 145 (1979); J. Badier et. al., CERN reports CERN-EP/80-36 and CERN-EP/80-147.

20. G. E. Hogan et. al., Phys. Rev. Lett. 42, 948 (1979).

21. See, e.g., J. Cardy and G. Windbow, Phys. Lett. 52B, 95 (1974); C. DeTar, S. D. Ellis, and P. Landshoff, Nucl. Phys. B87, 176 (1975); R. Doria, J. Frenkel, and J. C. Taylor, Nucl. Phys. B168, 93 (1980).

22. J. Collins, D. Soper, and G. Sterman, Phys. Lett. 109B, 388 (1982), and Stony Brook report ITP-SB-82-46 (1982), and XXI Int. Conf. on High Energy Physics, Paris, 1982. J. Collins, these proceedings.

23. G. Bodwin, S. Brodsky, and G. P. Lepage, Phys. Rev. Lett. 47, 1799 (1981) and SLAC report SLAC-PUB-2927, May, 1982. See also A. Mueller, Phys. Lett. 108B, 355 (1982). G. Bodwin, these proceedings.

24. W. W. Lindsay, D. Ross, and C. Sachrajda, Southampton report SHEP 81/82-6 (1982).

25. See also C. Michael and G. Wilk, Zeit. fur Physik C10, 169 (1981).

26. CERN NA3 collaboration, J. Badier et. al., Phys. Lett. 117B, 372 (1982).

27. European Muon Collaboration, K.-H. Becks, XXI Int. Conf. on High Energy Physics, Paris, 1982.

28. Michigan-Northeastern-Tufts-U. of Washington collaboration, S. R. Smith et. al., Phys. Rev. Lett. 46, 1607 (1981).

29. J. G. H. de Groot et. al., Phys. Lett. 82B, 456 (1979).

30. J. Kubar and F. Paige, Phys. Rev. D19, 221 (1978); G. Altarelli, R. K. Ellis, and G. Martinelli, Nucl. Phys. B157, 461 (1979); B. Humpert and W. L. Van Neervan, Phys. Lett. 89B, 69 (1979); K. Harada and T. Muta, Phys. Rev. D22, 663 (1980).

31. R. K. Ellis, Moriond Workshop on Lepton Pair Production, p.231; W. J. Stirling, these proceedings.

32. K. Harada, T. Kaneko, and N. Sakai, Nucl. Phys. B155, 169 (1979); J. Kubar, M. LeBellac, J. L. Meunier, and G. Plaut, Nucl. Phys. B175, 251 (1980).

33. G. Parisi, Phys. Lett. 90B, 295 (1980); G. Curci and M. Greco, Phys. Lett. 102B, 280 (1981); C. Korthals-Altes and E. DeRafael, Nucl. Phys.

B125, 275 (1977); A. Contogouris, S. Papadopoulos, and J. Ralston , Phys. Rev. D25, 1280 (1982).

34. P. Chiappetta, T. Grandou, M. LeBellac, and J. L. Meunier, Marseille report CPT-82/PE 1408 (1982).

35. L. Abbott, E. L. Berger, R. Blankenbecler, and G. Kane, Phys. Lett. 88B, 157 (1979); R. Blankenbecler, J. Gunion and P. Nason, SLAC report SLAC-Pub-2937 (1982).

36. E. L. Berger and S. J. Brodsky, Phys. Rev. Letters 42, 940 (1979); E. L. Berger, Zeit. für Physik C4, 289 (1980); S. J. Brodsky, these proceedings.

37. K. J. Anderson et. al., Phys. Rev. Lett. 43, 1219 (1979).

38. J. Badier et. al., Zeit. Phys. C11, 195 (1981); A. Michelini, CERN report CERN-EP/81-128 (1981). EPS Int. Conf. on High Energy Physics, Lisbon, July, 1981.

39. Chicago-Iowa-Princeton, Fermilab experiment E-615.

40. E. L. Berger and S. J. Brodsky, Phys. Rev. D24, 2428 (1981); E. L. Berger, Phys. Rev. D26, 105 (1982), and references therein; M. Haguenauer et. al., Phys. Lett. 100B, 185 (1981); C. Matteuzzi, SLAC-Pub 2827, DPF Annual Meeting, Santa Cruz, 1981.

41. Michigan-Northeastern-Tufts-Univ. of Washington collaboration, P. M. Mockett, Moriond Workshop on Lepton Pair Production, p.75.

42. Interesting data on associated hadrons are reported by D. Antreasyan et. al., Nucl. Phys. B199, 365 (1982), and by B. Pietrzyk et. al., CERN report CERN-EP/82-19 (1982). See also G. Bellettini, these proceedings.

43. R. K. Ellis, G. Martinelli, and R. Petronzio, Phys. Lett. 104B, 45 (1981) and Nucl. Phys. B211, 106 (1983).

44. F. Halzen and D. M. Scott, Phys. Rev.D24, 2433 (1981), and references therein.

45. W. Caswell, R. Horgan, and S. J. Brodsky, Phys. Rev. D18, 2415 (1978).

46. G. Altarelli, G. Parisi, R. Petronzio, Phys. Lett. 76B, 351 (1978) and 76B, 356 (1978).

47. Yu. Dokshitzer, D.Dyakanov, and S. Troyan, Phys. Rep. 58C, 269 (1980); G. Parisi and R. Petronzio, Nucl. Phys. B154, 427 (1979); S. Ellis and W. J. Stirling, Phys. Rev. D23, 214 (1981); G. Curci and M. Greco, Phys. Lett. 92B, 175 (1980); G. Curci, M. Greco, and Y. Srivastava, Nucl. Phys. B159, 451 (1979); C. Lo and J. Sullivan, Phys. Lett. 86B, 327 (1980); R. Odorico, Nucl. Phys. B199, 189 (1982); G. C. Fox and R. L. Kelly, Second Topical Forward Collider Conference, Madison, 1981; N. S. Craigie and H. F. Jones, Nucl. Phys. B172, 59 (1980); J. Kodaira and L. Trentadue, Phys. Lett. 112B, 66 (1982), and SLAC report SLAC-Pub-2934; J. C. Collins and D. Soper, Nucl. Phys. B193, 381 (1981), and Nucl. Phys. B197, 446 (1982); P. Rakow and B. R. Webber, Nucl. Phys. B187, 254 (1981).

48. For a recent review consult S. D. Ellis, Univ. of Washington report DOE/ER/40048-20-P2, XIII Int. Symp. on Multiparticle Dynamics, Volendam, 1982; M. Greco, these proceedings; W.-K. Tung, these proceedings.

49. G. C. Fox and S. Wolfram, Nucl. Phys. B168, 285 (1980) and Caltech report CALT-68-723; G. C. Fox, Caltech report CALT-68-683, 1981 SLAC Summer Institute.

50. P. Chiappetta and M. Greco, Marseille reports CPT 81/P.1307 (1981) and CPT 81/P.1335 (1981).

51. J. C. Collins and D. E. Soper, Moriond Workshop on Lepton Pair Production; D. Soper, these proceedings.

52. For more discussion see A. Buras, Proceedings of the 1981 International Symposium on Lepton and Photon Interactions at High Energies, (Bonn, 1981) Ed. by W. Pfeil; W. Celmaster and D. Sivers, Phys. Rev. D23, 227 (1981), and references therein.

FIGURE CAPTIONS

Fig. 1. Basic Drell-Yan $\bar{q}q$ annihilation process for $h_a h_b \to \gamma^* X$, with $\gamma^* \to \mu^+\mu^-$.

Fig. 2. (a) The $\bar{q}q \to \gamma^*$ subprocess and (b)-(h), some of the higher order perturbative QCD subprocesses which contribute to massive lepton pair production.

Fig. 3. (a) For $pN \to \gamma^* X$, the distribution $s d^2\sigma/dy\, d\sqrt{\tau}$ is plotted vs. $\sqrt{\tau}$ at $y = 0.2$ for $\sqrt{s} = 20$ GeV, and $\sqrt{s} = 60$ GeV. The calculation is performed with scale dependent structure functions obtained by the CDHS collaboration from fits to their ν and $\bar{\nu}$ data [Ref.5]. Here N denotes a target nucleus with 40% protons and 60% neutrons. (b) For $pp \to \gamma^* X$, $s d^2\sigma/dy\, d\sqrt{\tau}$ is plotted vs. $M/\sqrt{s}$ at $y = 0$ for $\sqrt{s} = 60$ GeV and $\sqrt{s} = 800$ GeV. (c) $s\, d^2\sigma/dy\, d\sqrt{\tau}$ is presented for γ^* production by antiproton beams: $\bar{p}p \to \gamma^* X$ at $y = 0$, for $\sqrt{s} = 15$ GeV and $\sqrt{s} = 60$ GeV.

Fig. 4(a). Experimental tests of scaling in $pN \to \gamma^* X$. The data are from Refs.6, 7, 17, and 18.

Fig. 4(b). Experimental tests of scaling in $\pi^- N \to \gamma^* X$. The data are from Refs.8 and 9.

Fig. 5. Data from various experiments show the growth of $\langle p_T \rangle$ as $\sqrt{s}$ is increased. This figure is taken from Kenyon, Ref.12.

Fig. 6. Figure taken from Kenyon's review, Ref.12. Shown are the γ^* decay angular distributions from three different experiments, ABCS, Ref.17, CHFMNP, Ref.7, and NA3, Ref.19.

Fig. 7. Initial state gluon exchanges are drawn between active and spectator constituents in πp scattering.

Fig. 8. Figure from Ref.31 showing the behavior of $K_{th}(\tau)$ in $pN \to \gamma^* X$ and $\pi^- N \to \gamma^* N$.

Fig. 9. The coefficient α from fits to $d\sigma/d\cos\theta = (1 + \alpha\cos\theta)$ is plotted as a function of x_F for $\pi^- N \to \gamma^* X$. The theoretical curve is from Ref.36. Data are from Ref.37 (CIP) and Ref.38 (NA3). If no high twist effects are present, the data should cluster about $\alpha \simeq 0.8$.

Fig. 10. Prediction from $O(\alpha_s)$ perturbative QCD for the slope b as a function of $M/\sqrt{s}$. This figure is taken from Ref.2.

Fig. 11. Data from the CERN NA3 Collaboration [Ref.26] showing the p_T dependence of $d\sigma/dp_T^2$ for $\pi^- N \to \gamma^* X$ at 3 values of the incident pion momentum.

Fig. 12. Comparison of a first order perturbative QCD computation of $Ed\sigma/d^3p$ with data from $pN \to \gamma^* X$ at $y = 0$ and $7 < M < 8$ GeV. The data are from Ref.6, and the theoretical curves are taken from Ref.2.

Fig. 13. A comparison of the calculated yield $d^2\sigma/dp_T^2 dM$ with data for $\pi^- N \to \gamma^* X$ at 150 GeV/c. The theoretical model includes soft gluon Sudakov effects and an ad-hoc intrinsic k_T distribution (from Ref.50).

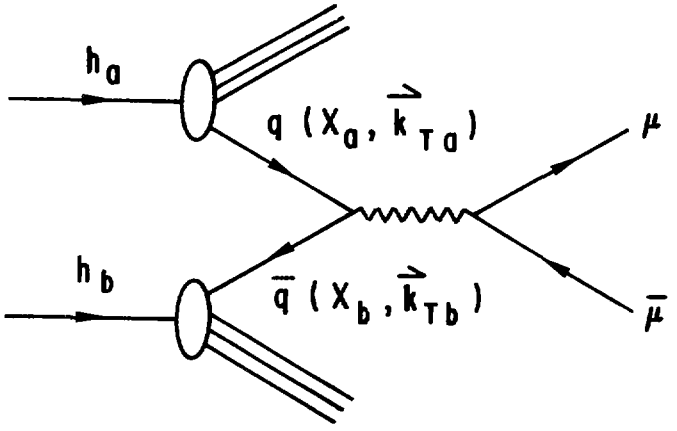

Fig. 1

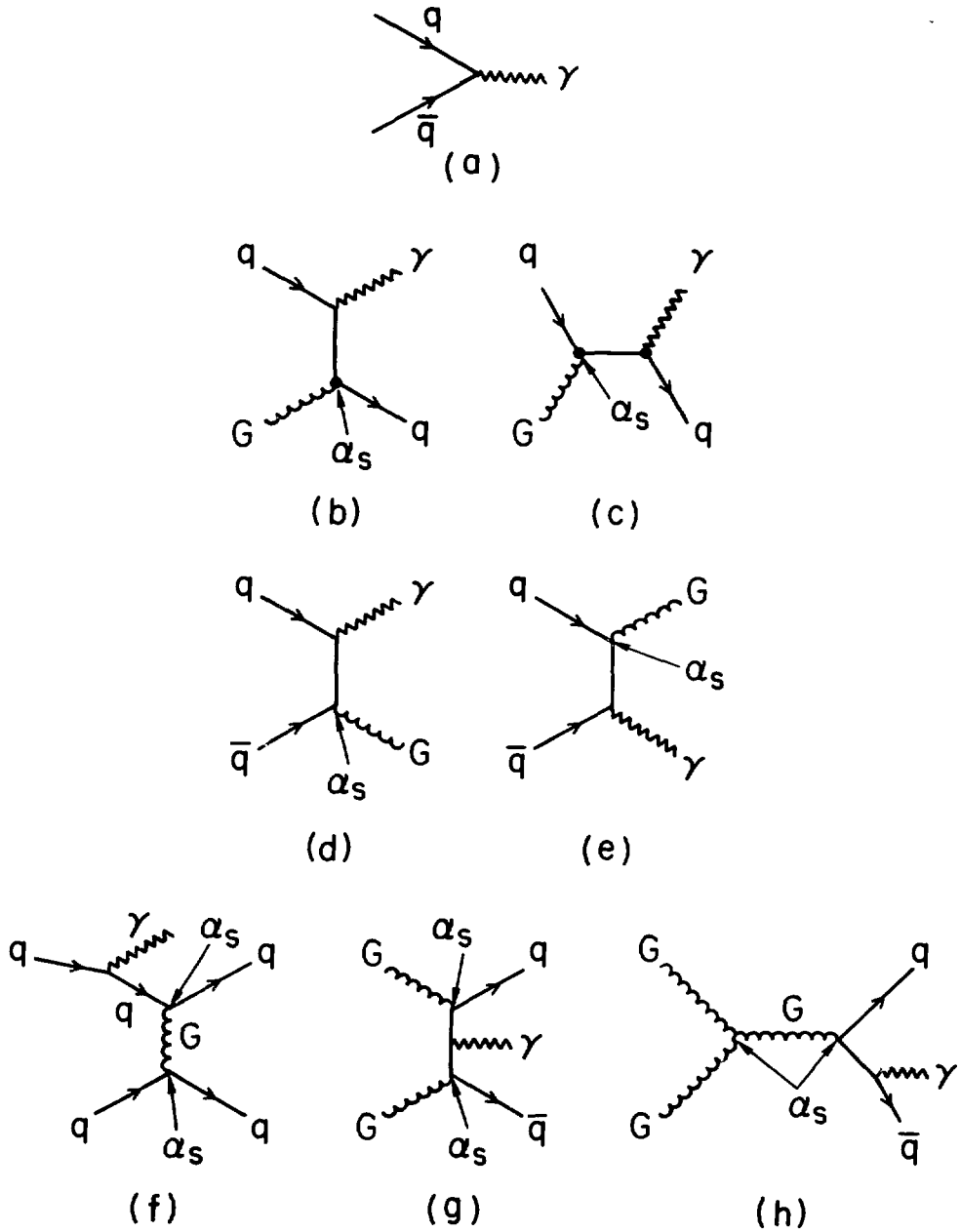
q
γ
q̄
(a)
q
γ
G
αs
q
(b)
q
γ
G
αs
q
(c)
q
γ
q̄
αs
G
(d)
q
G
αs
q̄
γ
(e)
γ
αs
q
q
G
q
q
αs
q
(f)
αs
G
q
γ
G
αs
q̄
(g)
G
q
G
γ
αs
G
q̄
(h)

Fig. 2

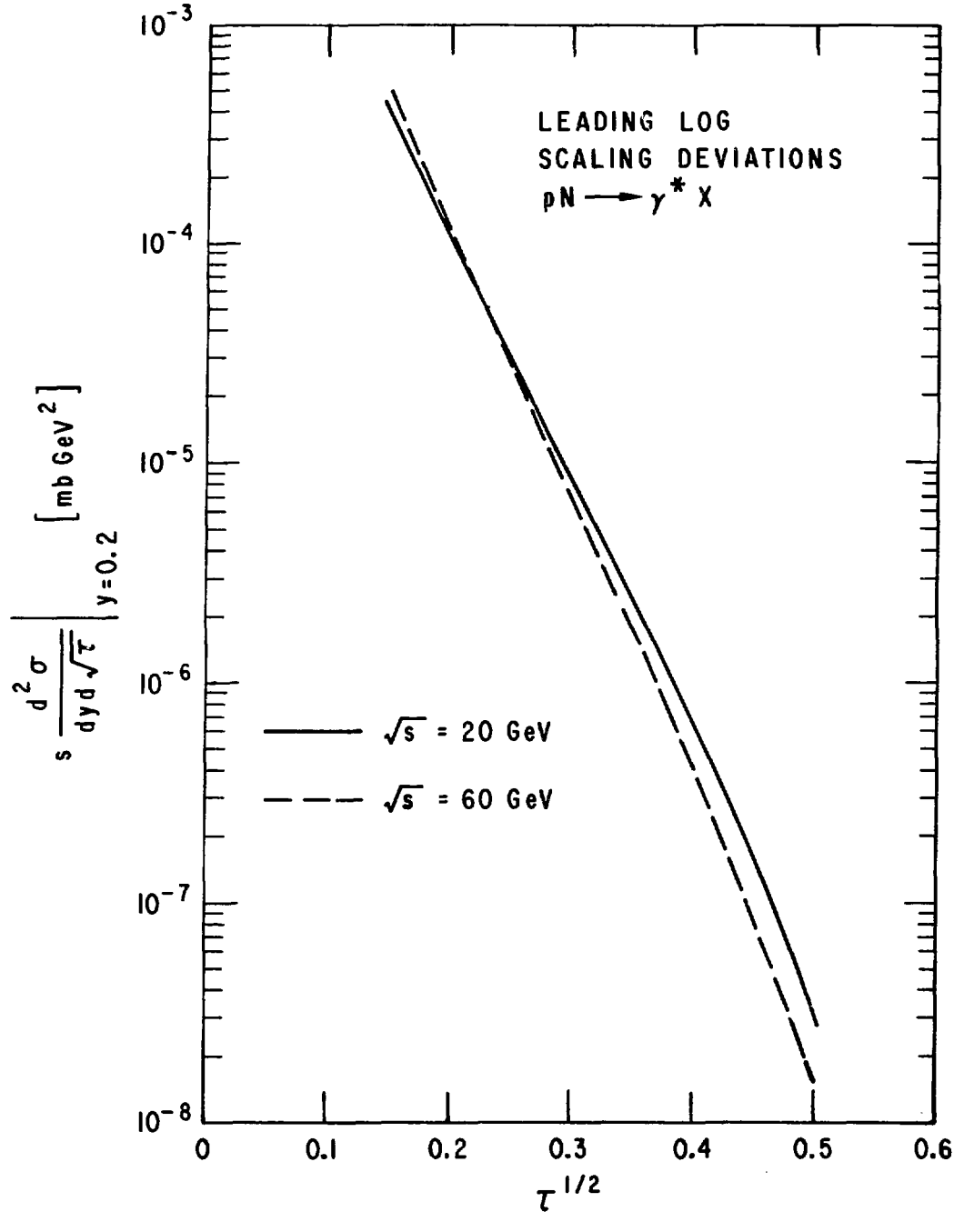
LEADING LOG
SCALING DEVIATIONS
pN → γ* X
√s = 20 GeV
√s = 60 GeV
$s \frac{d^2\sigma}{dy\, d\sqrt{\tau}}\Big|_{y=0.2}$ [mb GeV^2]
$\tau^{1/2}$
10^{-3}
10^{-4}
10^{-5}
10^{-6}
10^{-7}
10^{-8}
0
0.1
0.2
0.3
0.4
0.5
0.6

Fig. 3a

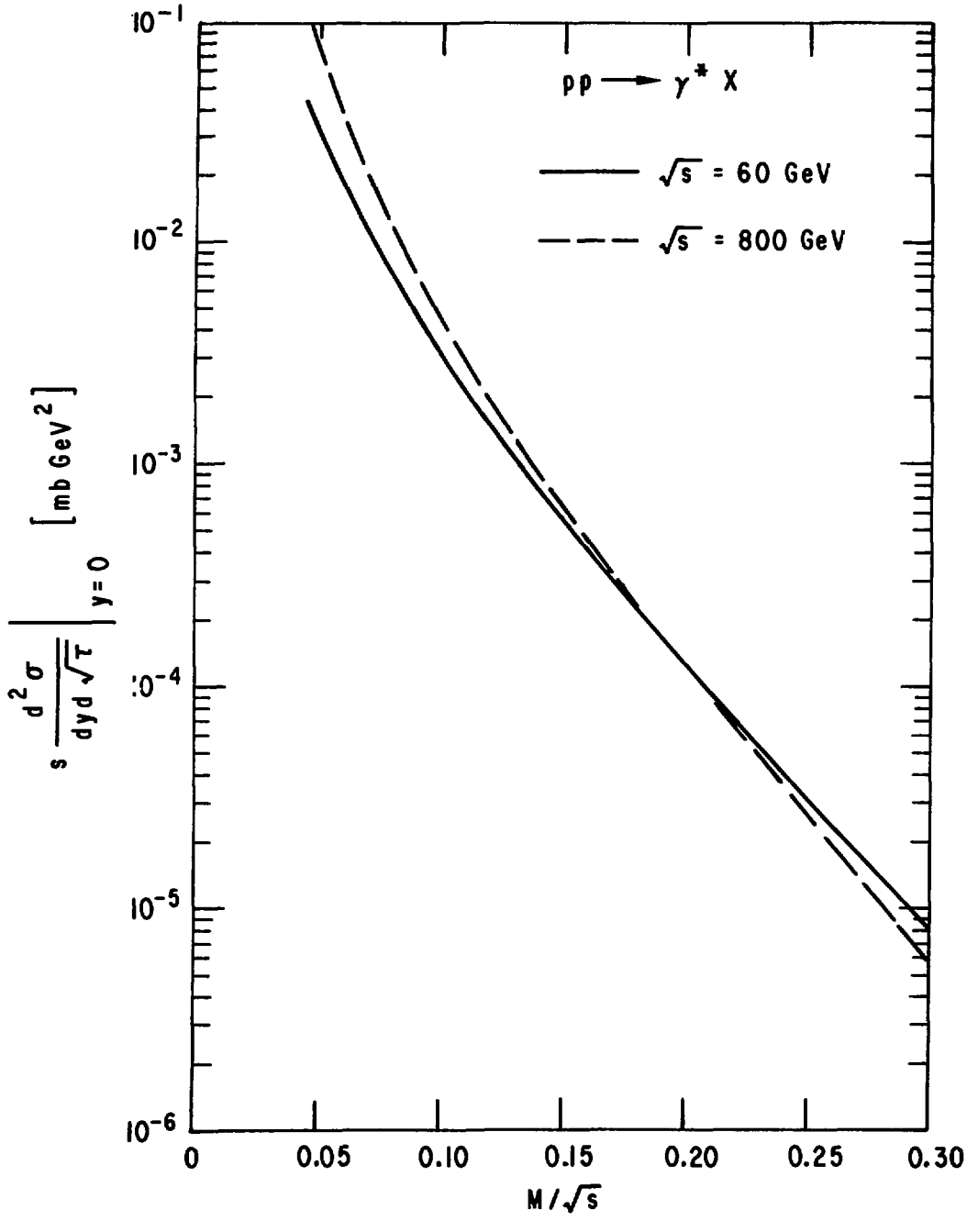
10^{-1}
10^{-2}
10^{-3}
10^{-4}
10^{-5}
10^{-6}
$pp \rightarrow \gamma^* X$
$\sqrt{s}$ = 60 GeV
$\sqrt{s}$ = 800 GeV
$s \frac{d^2\sigma}{dy d\sqrt{\tau}}\Big|_{y=0}$ [mb GeV^2]
0
0.05
0.10
0.15
0.20
0.25
0.30
$M/\sqrt{s}$

Fig. 3b

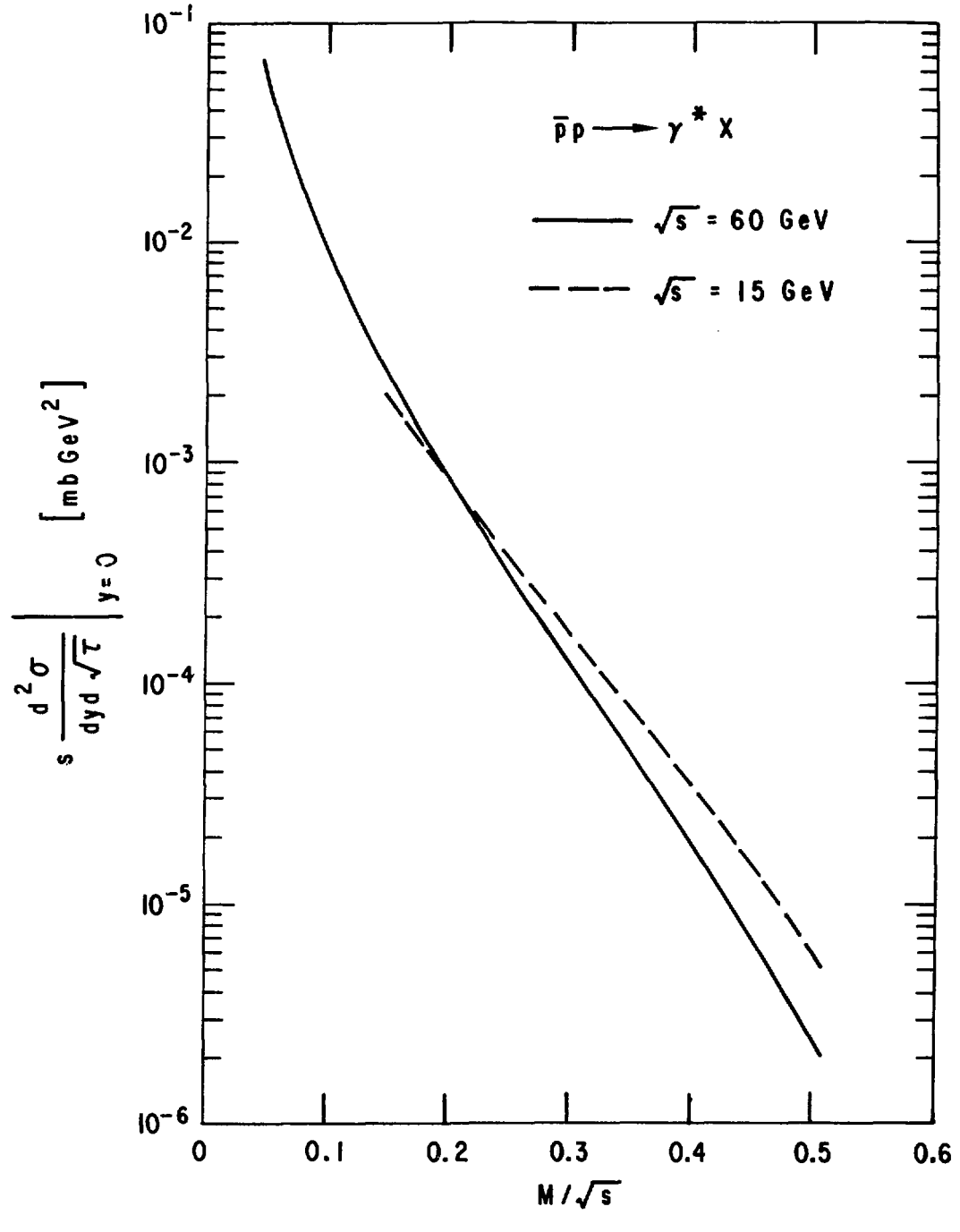
10^{-1}
10^{-2}
10^{-3}
10^{-4}
10^{-5}
10^{-6}
$\bar{p}p \longrightarrow \gamma^* X$
$\sqrt{s}$ = 60 GeV
$\sqrt{s}$ = 15 GeV
$s \frac{d^2\sigma}{dy d\sqrt{\tau}}\Big|_{y=0}$ [mb GeV^2]
0
0.1
0.2
0.3
0.4
0.5
0.6
$M/\sqrt{s}$

Fig. 3c

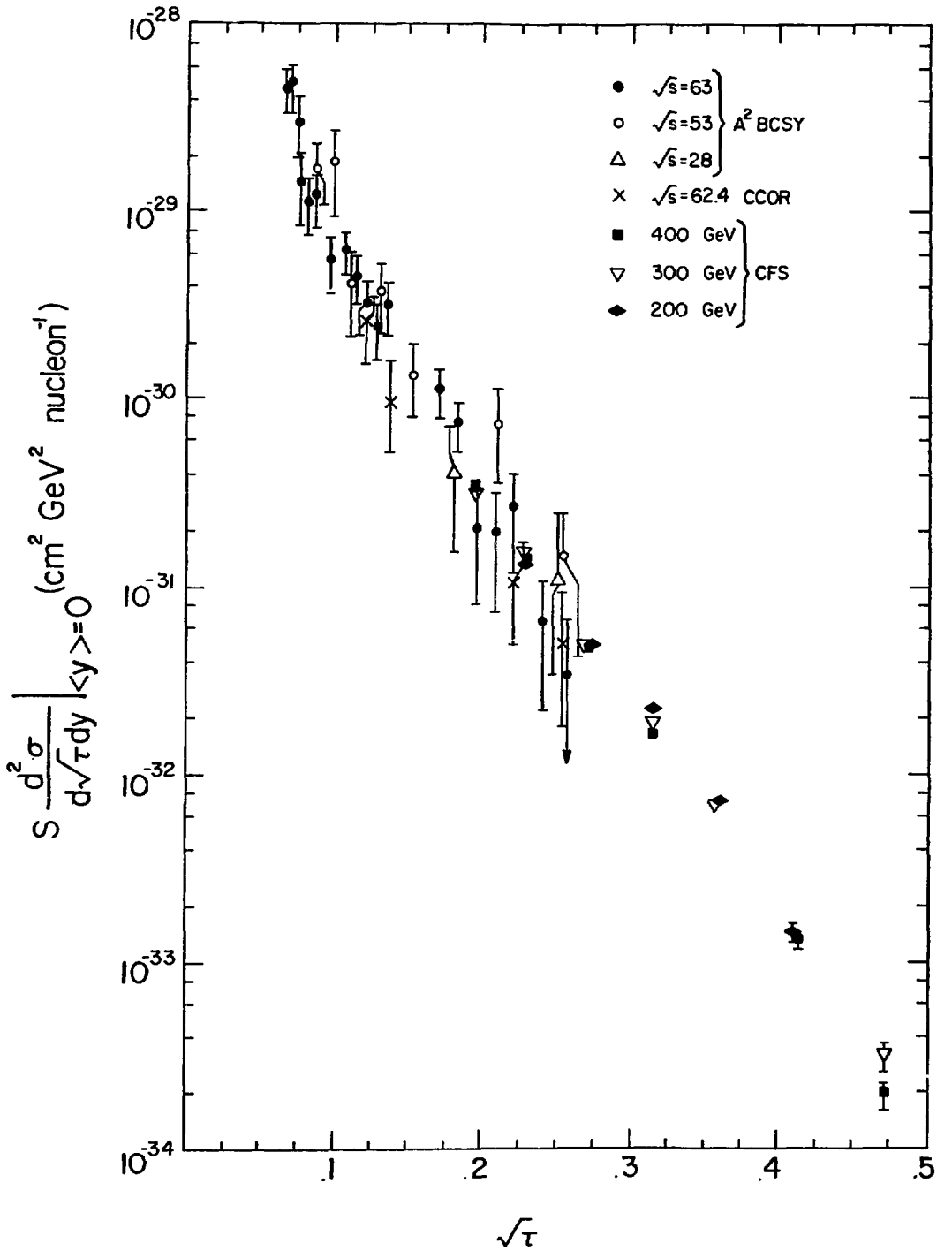
10^{-28}
10^{-29}
10^{-30}
10^{-31}
10^{-32}
10^{-33}
10^{-34}
.1
.2
.3
.4
.5
$\sqrt{\tau}$
$S\frac{d^2\sigma}{d\sqrt{\tau}dy}\Big|_{<y>=0}$ (cm^2 GeV^2 nucleon^{-1})
$\sqrt{s}$=63
$\sqrt{s}$=53
$\sqrt{s}$=28
A^2 BCSY
$\sqrt{s}$=62.4 CCOR
400 GeV
300 GeV
200 GeV
CFS

Fig. 4a

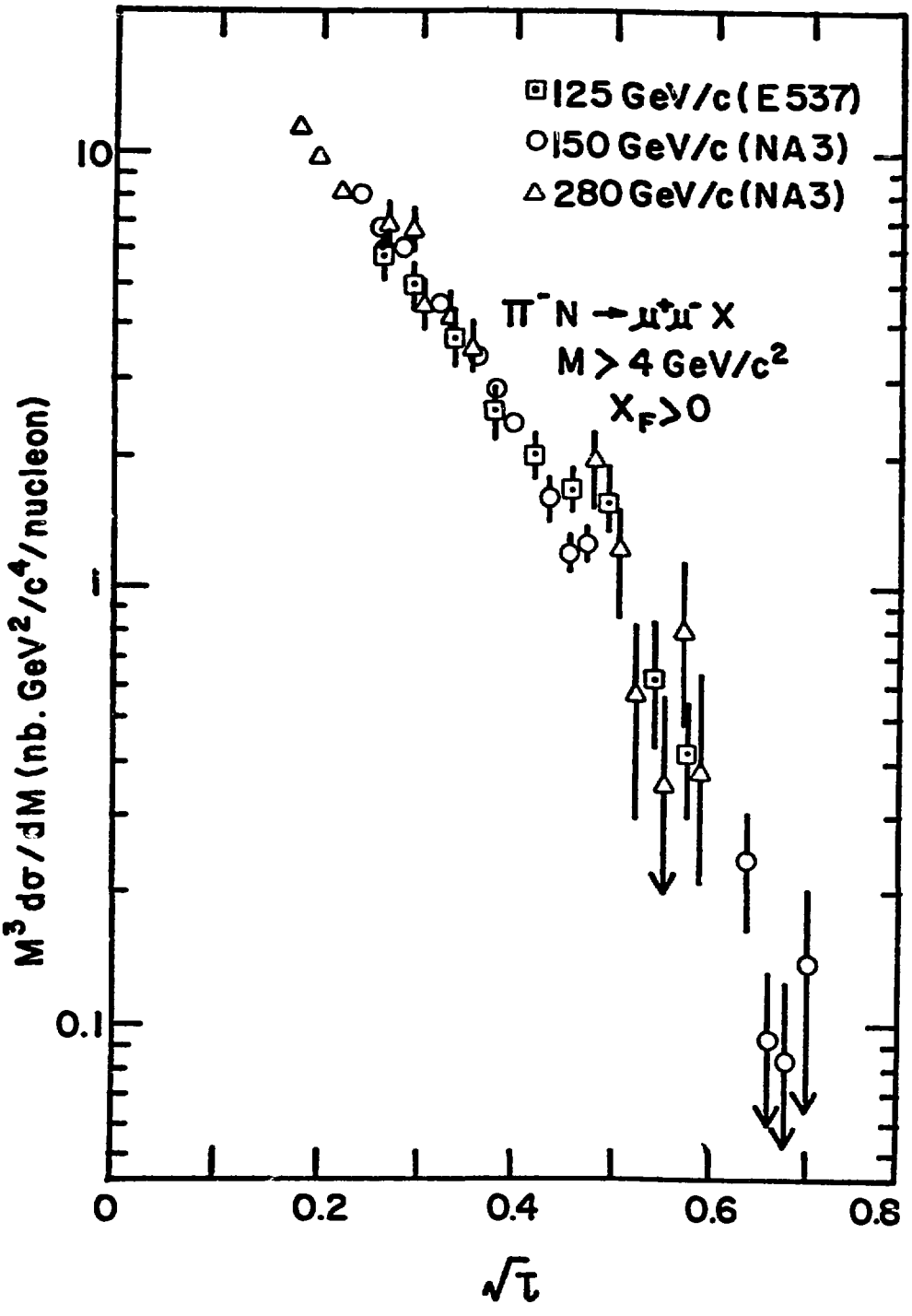
125 GeV/c (E537)
150 GeV/c (NA3)
280 GeV/c (NA3)
π⁻N → μ⁺μ⁻X
M > 4 GeV/c²
X_F > 0
M³ dσ/dM (nb. GeV²/c⁴/nucleon)
10
1
0.1
0
0.2
0.4
0.6
0.8
√τ

Fig. 4b

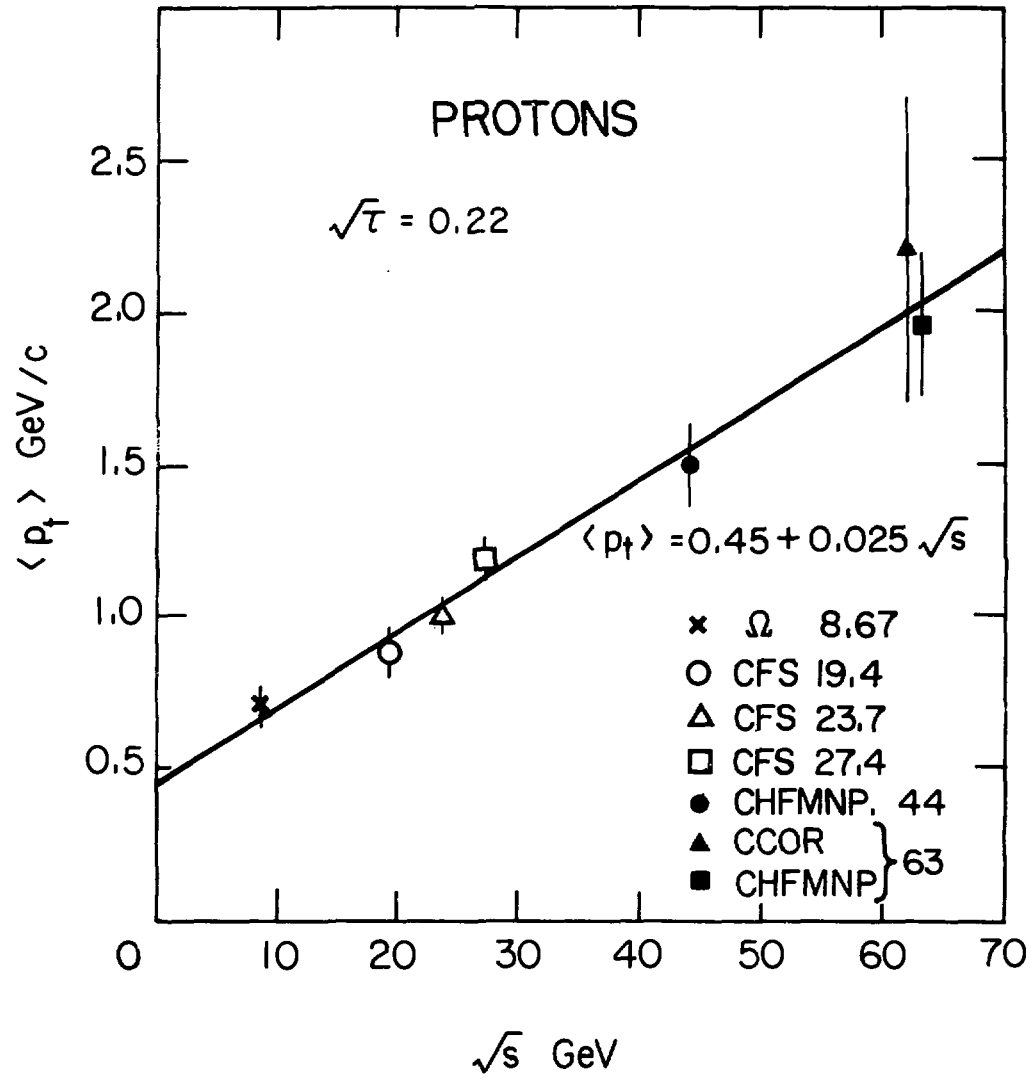
PROTONS
$\sqrt{\tau}$ = 0.22
$\langle p_t \rangle$ = 0.45 + 0.025 $\sqrt{s}$
× Ω 8.67
○ CFS 19.4
△ CFS 23.7
□ CFS 27.4
● CHFMNP, 44
▲ CCOR
■ CHFMNP
63
$\langle p_t \rangle$ GeV/c
$\sqrt{s}$ GeV
0
10
20
30
40
50
60
70
0.5
1.0
1.5
2.0
2.5

Fig. 5

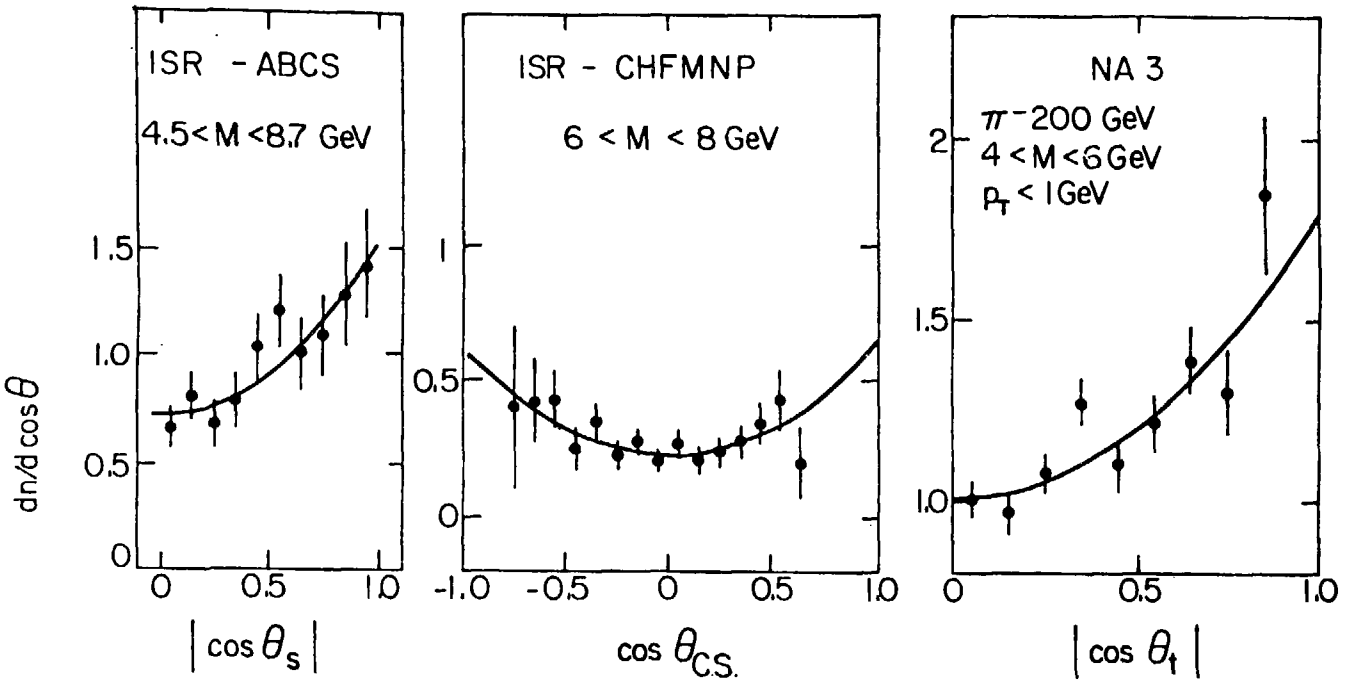
ISR - ABCS
4.5< M <8.7 GeV
ISR - CHFMNP
6 < M < 8 GeV
NA 3
π⁻ 200 GeV
4 < M < 6 GeV
p_T < 1 GeV
dn/d cos θ
| cos θ_s |
cos θ_CS.
| cos θ_t |

Fig. 6

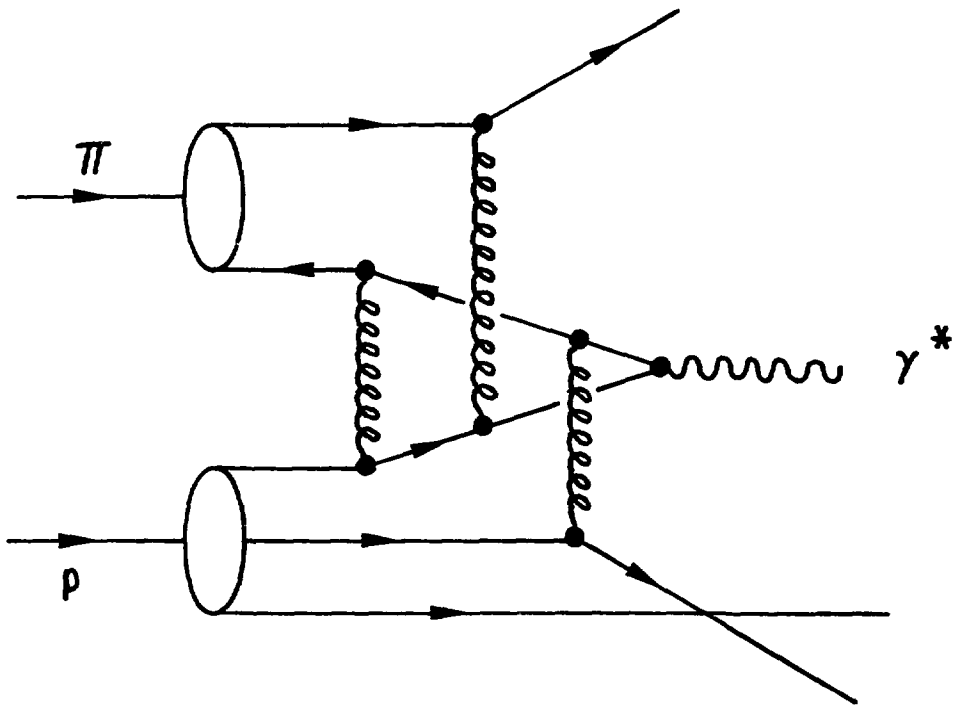

Fig. 7

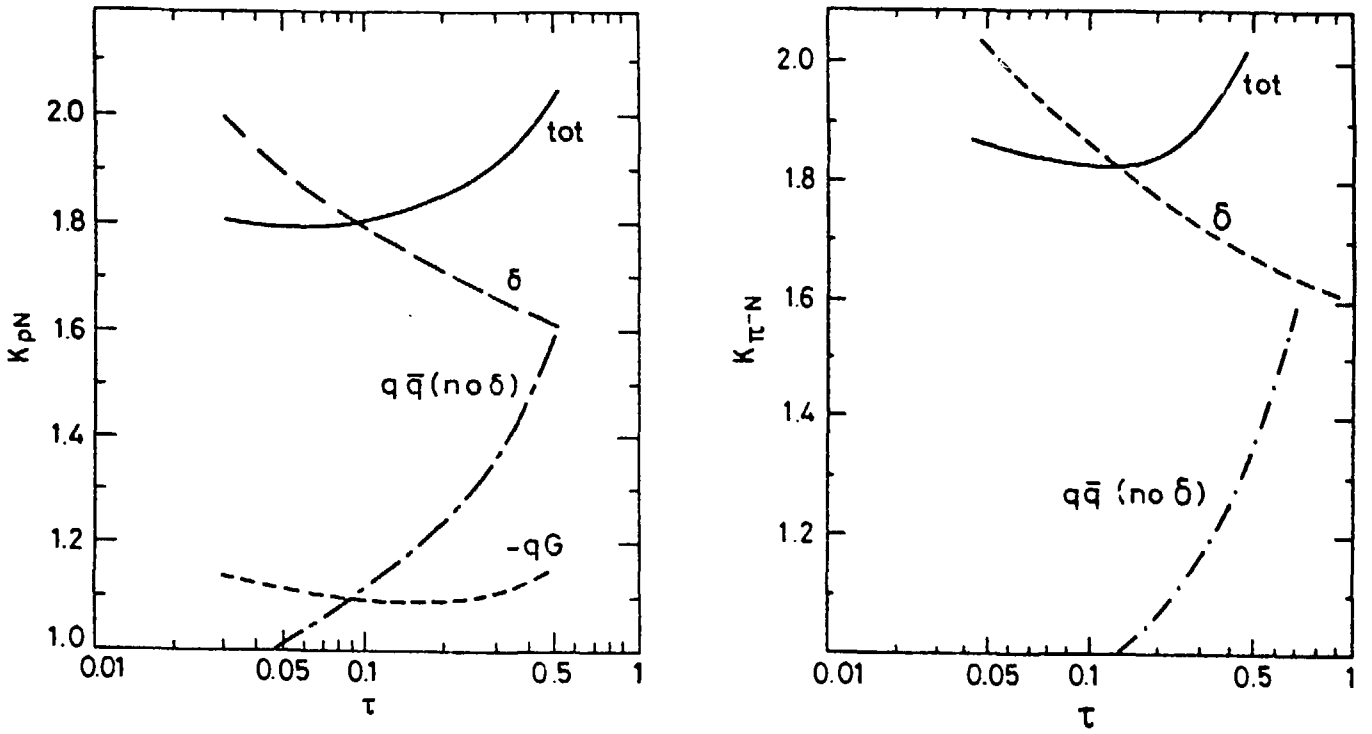
2.0
1.8
1.6
1.4
1.2
1.0
$K_{\rho N}$
tot
δ
q q̄ (no δ)
-qG
0.01
0.05
0.1
0.5
1
τ
2.0
1.8
1.6
1.4
1.2
$K_{\pi^- N}$
tot
δ
qq̄ (no δ)
0.01
0.05
0.1
0.5
1
τ

Fig. 8

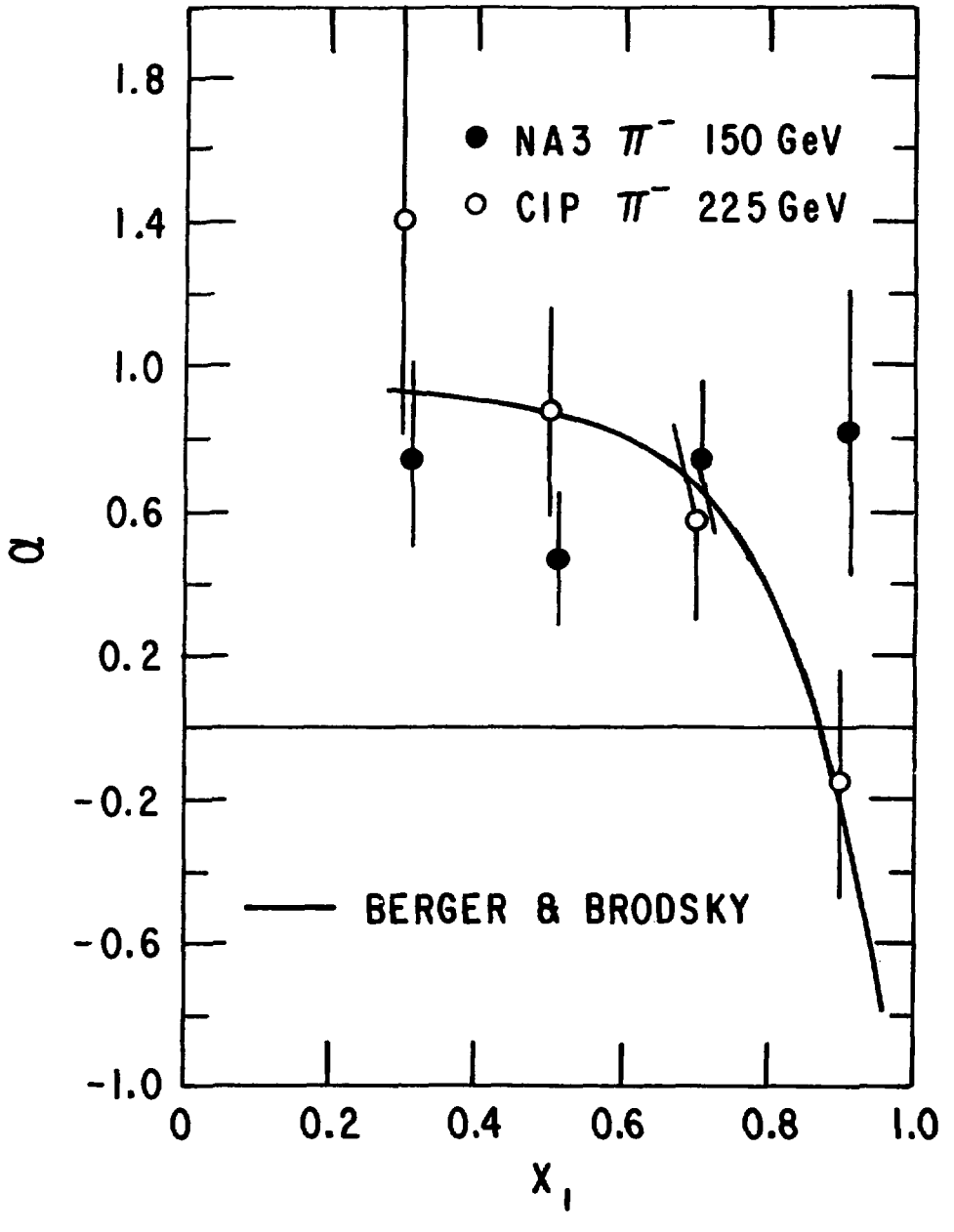
1.8
1.4
1.0
0.6
0.2
-0.2
-0.6
-1.0
α
0
0.2
0.4
0.6
0.8
1.0
X_1
NA3 π^- 150 GeV
CIP π^- 225 GeV
BERGER & BRODSKY

Fig. 9

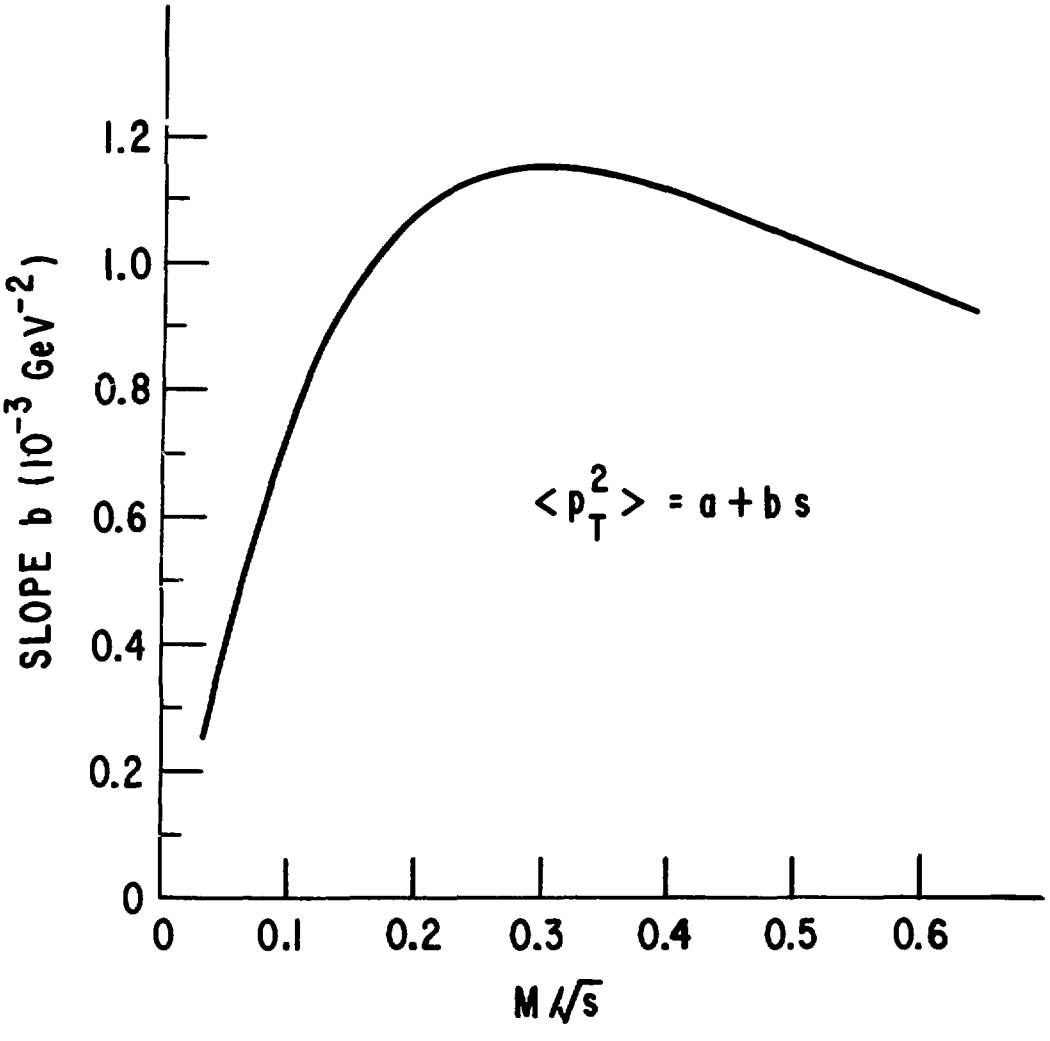
SLOPE b (10^{-3} GeV^{-2})
1.2
1.0
0.8
0.6
0.4
0.2
0
$\langle p_T^2 \rangle = a + b\,s$
0
0.1
0.2
0.3
0.4
0.5
0.6
$M/\sqrt{s}$

Fig. 10

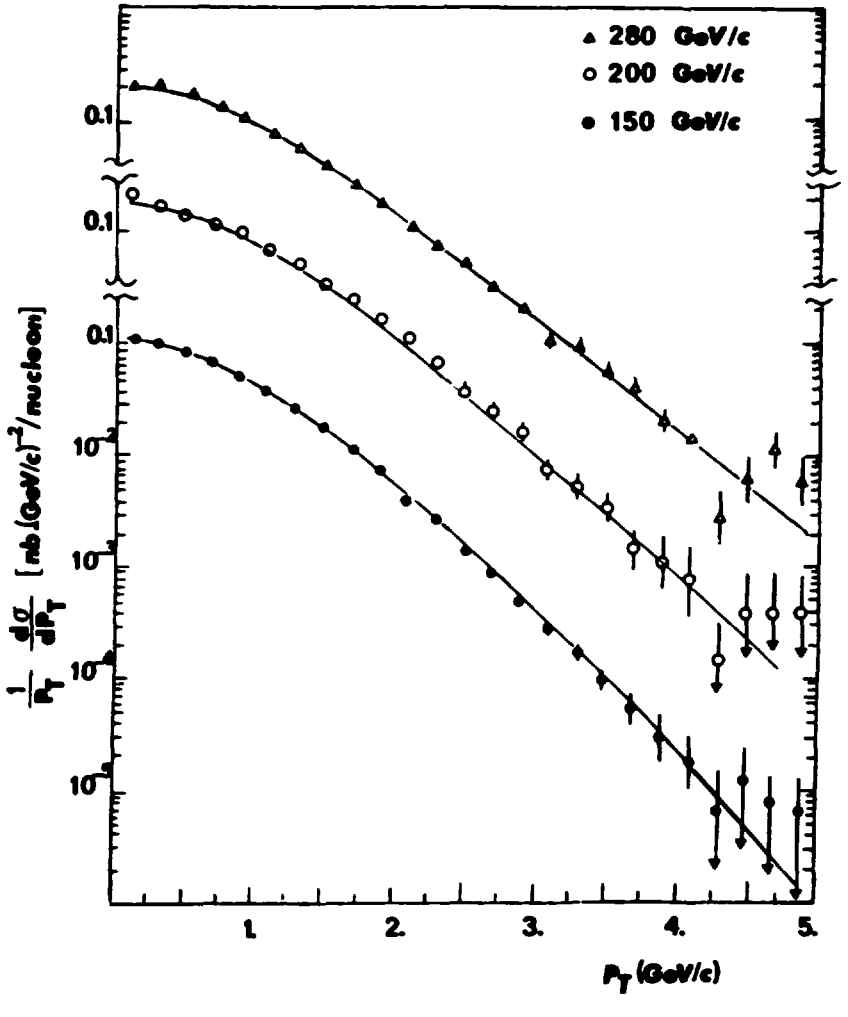
▲ 280 GeV/c
○ 200 GeV/c
● 150 GeV/c
0.1
0.1
0.1
10^{-2}
10^{-3}
10^{-4}
$\frac{1}{P_T}\frac{d\sigma}{dP_T}$ [nb/(GeV/c)^2/nucleon]
1.
2.
3.
4.
5.
P_T (GeV/c)

Fig. 11

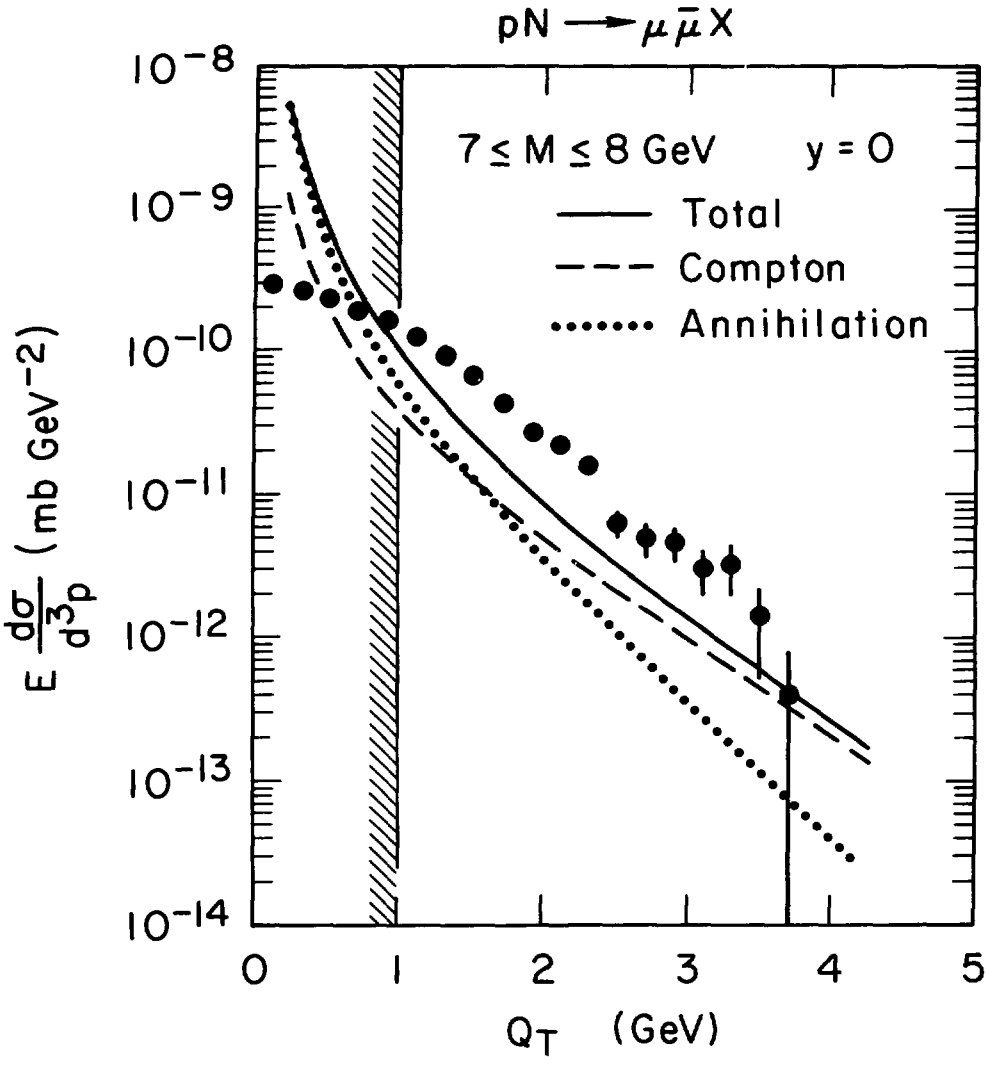
pN → μμ̄X
7 ≤ M ≤ 8 GeV
y = 0
Total
Compton
Annihilation
E dσ/d³p (mb GeV⁻²)
10⁻⁸
10⁻⁹
10⁻¹⁰
10⁻¹¹
10⁻¹²
10⁻¹³
10⁻¹⁴
0
1
2
3
4
5
Q_T (GeV)

Fig. 12

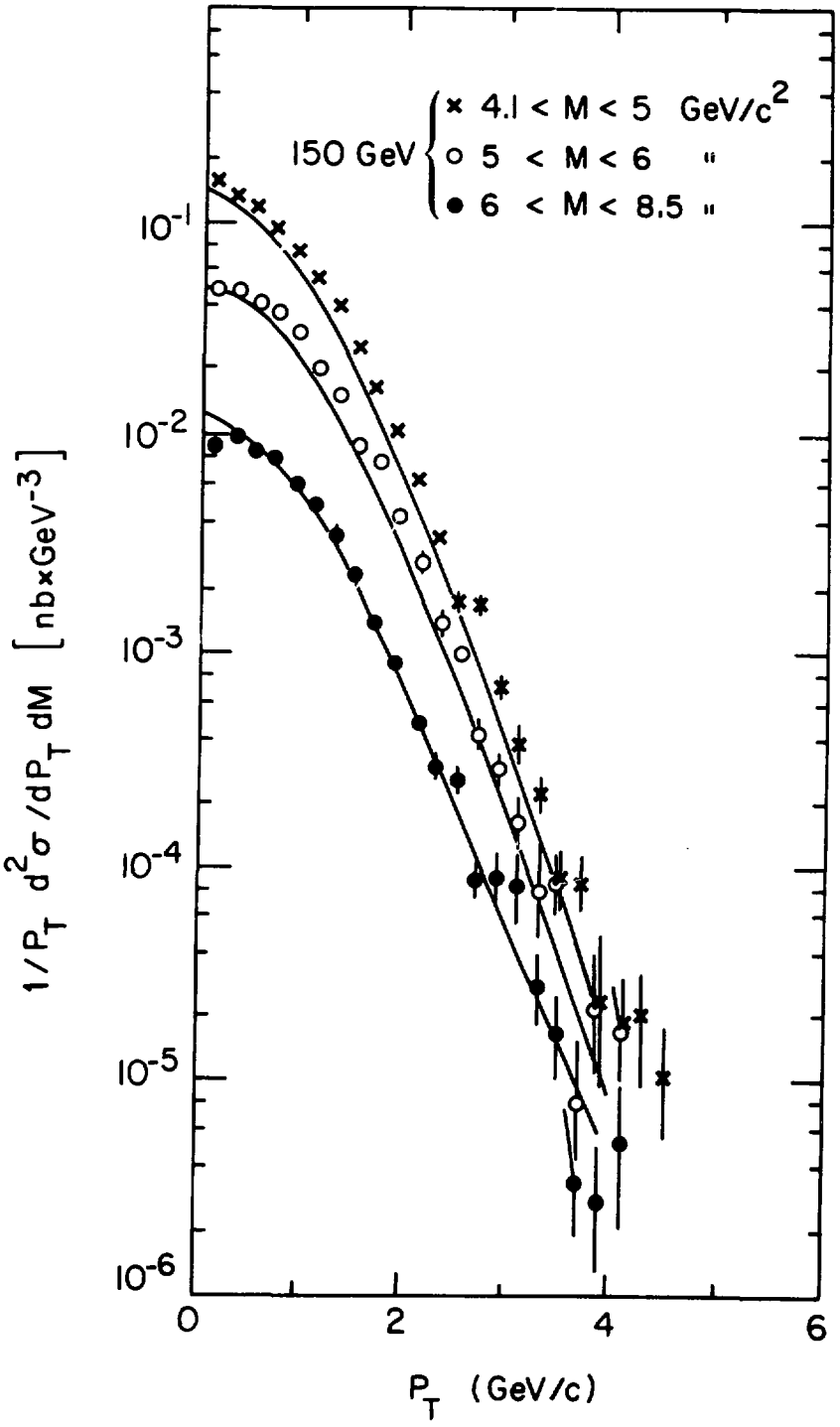
150 GeV
× 4.1 < M < 5 GeV/c²
○ 5 < M < 6 "
● 6 < M < 8.5 "
10⁻¹
10⁻²
10⁻³
10⁻⁴
10⁻⁵
10⁻⁶
0
2
4
6
1/P_T d²σ/dP_T dM [nb×GeV⁻³]
P_T (GeV/c)

Fig. 13

DISCLAIMER